

Max-Min Fairness for Stacked Intelligent Metasurface-Assisted Multi-User MISO Systems

Nipuni Ginige (*Graduate Student Member, IEEE*), Prathapasinghe Dharmawansa, Arthur Sousa de Sena (*Member, IEEE*), Nurul Huda Mahmood (*Member, IEEE*), Nandana Rajatheva (*Senior Member, IEEE*) and Matti Latva-aho (*Fellow, IEEE*)

Abstract—Stacked intelligent metasurface (SIM) is an emerging technology that uses multiple reconfigurable surface layers to enable flexible wave-based beamforming. In this paper, we focus on an SIM-assisted multi-user multiple-input single-output system, where it is essential to ensure that all users receive a fair and reliable service level. To this end, we develop two max-min fairness algorithms based on instantaneous channel state information (CSI) and statistical CSI. For the instantaneous CSI case, we propose an alternating optimization algorithm that jointly optimizes power allocation using geometric programming and wave-based beamforming coefficients using the gradient descent-ascent method. For the statistical CSI case, since deriving an exact expression for the average minimum achievable rate is analytically intractable, we derive a tight upper bound and thereby formulate a stochastic optimization problem. This problem is then solved, capitalizing on an alternating approach combining geometric programming and gradient descent algorithms, to obtain the optimal policies. Our numerical results show significant improvements in the minimum achievable rate compared to the benchmark schemes. In particular, for the instantaneous CSI scenario, the individual impact of the optimal wave-based beamforming is significantly higher than that of the power allocation strategy. Moreover, the proposed upper bound is shown to be tight in the low signal-to-noise ratio regime under the statistical CSI.

Index Terms—Alternating optimization, geometric programming, gradient descent-ascent, max-min fairness, stacked intelligent metasurfaces, statistical CSI, wave-based beamforming.

I. INTRODUCTION

STACKED intelligent metasurface (SIM) is a novel technology that uses multiple (refractive) reconfigurable intelligent surface (RIS) layers to enable wave-domain beamforming [1]–[5]. By manipulating electromagnetic waves at the analog level, SIM eliminates the need for conventional digital precoding, thus reducing processing delays [1], [3]. Moreover, SIM-based transceivers require fewer radio frequency (RF) chains, leading to lower hardware costs and energy consumption compared to traditional massive multiple-input multiple-output (MIMO) systems [2], [3].

The transmit beamforming waveform of SIM-aided systems needs to be optimised to reap the full advantages of

its benefits. Mathematical optimization has been essential in wireless communication systems from first-generation (1G) to fifth-generation (5G) and will continue to be crucial in the upcoming sixth-generation (6G) [6]. Usually, optimization involves tuning the transmission parameters, such as the transmit power, transmit beamformers, RIS phase shifts, etc., with the aim of maximizing (or minimizing) one or more objective functions like the sum rate, system throughput, or spectral efficiency while effectively managing interference [7]–[10]. However, maximizing a given performance measure may result in unfair allocation where users with favorable conditions are prioritized over users in disadvantageous situations, such as cell edge users. In particular, max-min fairness is a widely used strategy to allocate resources efficiently, prioritizing weaker users without unnecessary waste [11].

Developing specialized schemes to enhance fairness by maximizing the minimum rate or signal-to-interference-plus-noise ratio (SINR) is essential for SIM-assisted networks, as their multilayer architecture presents unique optimization challenges that demand dedicated solutions [12], [13]. In this regard, mathematical optimization is key, facilitating the joint optimization of power allocation and wave-based beamforming to fully harness the benefits of SIM technology. Usually, resource optimization requires instantaneous channel state information (CSI), which incurs signaling overhead and practical limitations. Therefore, leveraging statistical CSI reduces computational and signaling overhead compared to instantaneous CSI, making SIM optimization more practical for real-world applications [14]. Although recent studies have focused on optimization techniques for SIM-assisted networks targeting different objectives, ensuring fair resource allocation among users has remained largely unaddressed. Moreover, to the best of our limited knowledge, fairness-based resource optimization under statistical CSI constraints has not been addressed in the literature either. The next section reviews relevant related works.

A. RELATED WORKS

Ample recent works on SIM-assisted wireless networks have focused on power allocation and wave-based beamforming to maximize achievable sum rate or spectral efficiency [14]–[20]. The authors of [15] proposed a SIM-based transceiver design for a multiple-input single-output (MISO) downlink system. They formulated an optimization problem to iteratively determine the optimal power allocation

Nipuni Ginige, Prathapasinghe Dharmawansa, Arthur S. de Sena, Nurul H. Mahmood, Nandana Rajatheva, and Matti Latva-aho are with the Center for Wireless Communications, University of Oulu, 90570 Oulu, Finland (e-mail: nipuni.ginige@oulu.fi, pkaluwad24@univ.yo.oulu.fi, arthur.sena@oulu.fi, nurulhuda.mahmood@oulu.fi, nandana.rajatheva@oulu.fi, matti.latva-aho@oulu.fi).

This work was supported by 6G Flagship (Grant Number 369116) funded by the Research Council of Finland.

and wave-based beamforming to maximize the system's sum rate. An iterative water-filling algorithm was used for power allocation, while a projected gradient ascent algorithm and a successive refinement method were applied to address the beamforming problem. In [16], an iterative projected gradient approach was applied to jointly optimize the transmit covariance matrix and RIS phase shifts, which maximized the achievable rate in a multi-stream holographic MIMO system with SIM. Similarly, [17] proposed a SIM-enhanced fully analog wideband beamforming design that approximated the end-to-end channel as a diagonal matrix by optimizing RIS phase shifts. A deep reinforcement learning-based method was introduced in [18], [19] to jointly optimize transmit power allocation and wave-based beamforming in a SIM-assisted multi-user MIMO system. The authors of [20] proposed an optimal resource allocation algorithm while maximizing the sum rate for SIM-assisted systems with both phase control and amplitude control layers. In [21], a SIM-enhanced cell-free massive MIMO system was presented along with a greedy-based pilot allocation algorithm, an iterative optimization algorithm for wave-based beamforming, and a max-min spectral efficiency power control algorithm using a bisection method. Moreover, [22] proposed an algorithm that optimized wave-based beamforming by maximizing the sum rate and shaping the sensing beam pattern with a dual-normalized differential gradient descent.

Max-min fairness optimization was also extensively studied for conventional RIS-assisted systems. In [23], max-min fairness in a group-transmissive RIS-assisted downlink system was addressed using successive convex approximation and semi-definite relaxation (SDR). The work in [24] maximized the minimum weighted SINR—subject to individual transmit power and RIS reflection constraints—using second-order cone programming (SOCP) and SDR. An optimal linear precoder was employed in [25] to maximize the minimum SINR under a power constraint. In [26], a max-min fairness algorithm was developed for optimizing active-passive beamforming and power allocation in RIS-assisted non-orthogonal multiple access systems, using block coordinate descent and limited-memory Broyden-Fletcher-Goldfarb-Shanno algorithms. The work in [27] considered max-min rate optimization for RIS-assisted cell-free systems by optimizing transmit power and phase shifts with geometric programming (GP) and SDR. In [28], max-min SINR optimization was investigated under users' maximum allowable electromagnetic exposure. In addition, [29] proposed a convex-hull relaxation for the discrete phase shift constraint and solved the reformulated problem using an alternating projection/proximal gradient descent and ascent algorithm. Finally, [30] applied a gradient descent-ascent (GDA)-based approach along with SDR to solve the max-min signal-to-noise ratio (SNR) problem in a multi-user RIS-assisted system.

To reduce computational overhead, several studies employed statistical CSI-based optimization. In [14], transmit power and RIS phase shifts were optimized based on statistical CSI to improve rate performance in SIM-assisted MIMO systems, using the use-and-then-forget bound for downlink spectral efficiency. The work in [31] derived an approximate closed-

form expression for the achievable uplink net rate of a RIS-assisted cell-free system using statistical CSI, then solved the max-min SINR problem by jointly optimizing receiver filter coefficients, power allocations, and RIS phase shifts through closed-form solutions, GP, and alternating maximization. In [32], the performance of a simultaneously transmitting and reflecting RIS in a massive MIMO downlink system with hardware impairments was examined using an optimal linear precoder and a passive beamforming matrix to maximize the minimum SINR, with amplitude and phase shifts optimized via a projected gradient ascent algorithm based on statistical CSI. Similarly, [33] investigated transmit power allocation and phase shift optimization based on statistical CSI while ensuring user fairness by maximizing the sum of eigenvalues of the composite channel's correlation matrix through an iterative algorithm and GP. An upper bound on the ergodic spectral efficiency for RIS-assisted systems was derived in [34], with RIS phase shifts optimized using SDR and Gaussian randomization. In [35], an approximate closed-form expression for the uplink ergodic data rate was derived and a genetic algorithm was used for phase shift optimization. Finally, [36] obtained an approximate closed-form expression of the ergodic sum rate and addressed the joint active-passive beamforming problem using deep reinforcement learning.

B. MOTIVATION AND CONTRIBUTIONS

As discussed, existing studies on SIM-assisted wireless networks have primarily focused on maximizing the achievable sum rate or spectral efficiency. To the best of our knowledge, the max-min fairness problem in these systems remains unexplored. Ensuring fairness is crucial to guarantee that all users receive a reasonable quality of service, especially in multi-user scenarios. Additionally, optimizing resource allocation based on statistical CSI reduces computational overhead by eliminating the need for frequent re-optimization. However, this approach has yet to be investigated in the context of max-min fairness for SIM-assisted systems. Motivated by this gap, we develop a max-min fairness algorithm for SIM-assisted multi-user MISO systems that jointly optimizes power allocation and wave-based beamforming using both instantaneous and statistical CSI. Our main contributions are as follows:

- This paper proposes two novel max-min fairness algorithms for SIM-assisted multi-user MISO downlink systems. One algorithm is designed for instantaneous CSI, while the other is based on statistical CSI. Both approaches iteratively optimize power allocation and wave-based beamforming to improve fairness among users. Specifically, we assume the perfect CSI knowledge in every coherence interval during optimization with instantaneous CSI and the knowledge of channel characteristics for a selected period of coherence intervals during optimization with statistical CSI.
- For the instantaneous CSI case, we formulate an optimization problem to maximize the minimum SINR, subject to the total transmit power budget and the practical constraint of discrete phase shifts. To solve this problem, we propose an alternating optimization algorithm

that iteratively updates power allocation and wave-based beamforming. Specifically, GP is used to refine power allocation for a given wave-based beamforming matrix, while a GDA-based method adjusts the beamforming for a fixed power allocation.

- For the statistical CSI case, we formulate an optimization problem based on a bound on the average minimum achievable rate, as the exact average rate is analytically intractable. To address this, we develop an alternating optimization algorithm that combines geometric programming for power allocation with a gradient-descent-based method for wave-based beamforming.
- Finally, we provide simulation results to evaluate the performance of the proposed max-min fairness optimization algorithms. The results show that our approach achieves an order of magnitude higher minimum rate and higher fairness compared to equal power allocation and random phase shift assignment with instantaneous CSI. Moreover, while both power allocation and wave-based beamforming improve performance, the latter has a more significant impact. Furthermore, the results confirm that the proposed upper bound on the average minimum achievable rate remains tight in the low-SNR regime with statistical CSI.

The rest of the paper is organized as follows. The system model for the SIM-assisted system is described in Section II. In Section III, we present the proposed max-min fairness optimization algorithm based on instantaneous CSI, while in Section IV, we present the proposed max-min fairness optimization algorithm based on statistical CSI. The numerical results are presented in Section V, and Section VI concludes our paper.

Notations: Lowercase letters represent scalars, boldface lowercase letters denote column vectors, and boldface uppercase letters represent matrices. Moreover, $|z|$, $\Re(z)$, and $\Im(z)$ denote the absolute value, real part, and imaginary part of a complex number z , respectively. j is the imaginary unit which satisfies $j^2 = -1$. The notations for the transpose, the Hermitian transpose and the Euclidean norm of \mathbf{A} are given by \mathbf{A}^T , \mathbf{A}^H , and $\|\mathbf{A}\|_2$, respectively. The operator $\text{diag}(\cdot)$ transforms a vector into a diagonal matrix. \mathbf{I}_N is the $N \times N$ identity matrix. The square root of a positive-definite/ positive-semi-definite matrix is denoted by $(\cdot)^{1/2}$. The mathematical expectation is denoted by $\mathbb{E}\{\cdot\}$. Additionally, $\mathbf{1}$ and $\mathbf{0}$ represent the all-one vector and the all-zero vector, respectively. Moreover, $\text{sinc}(x) = \frac{\sin(\pi x)}{\pi x}$ is the sinc function and $\frac{\partial f}{\partial x}$ is the partial derivative of a function f with respect to x . Finally, $\lfloor \cdot \rfloor$ represents the floor operator and $\log_a(\cdot)$ is the logarithmic function with base a .

II. SYSTEM MODEL

We consider in this work a downlink SIM-assisted multi-user MISO system, as shown in Fig. 1, where one base station (BS) employing N transmit antennas is assisted by a SIM and communicates with K single-antenna user equipments (UEs). The SIM is made with L metasurface layers and positioned near the BS antennas. Each SIM layer comprises M scattering

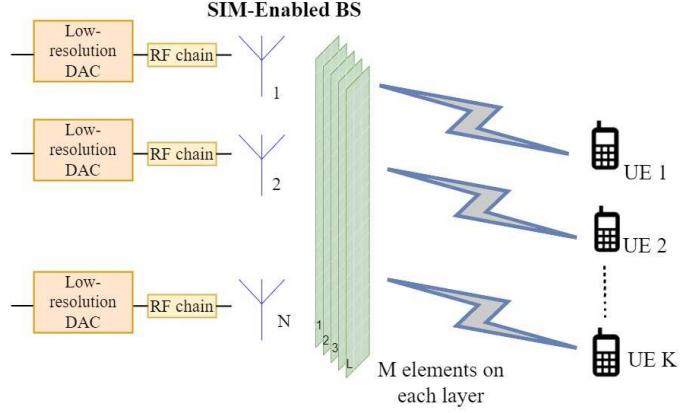


Fig. 1. SIM-assisted communication system.

elements. Let $\mathcal{L} = \{1, \dots, L\}$, $\mathcal{M} = \{1, \dots, M\}$ and $\mathcal{K} = \{1, \dots, K\}$ denote the sets of metasurface layers, scattering elements on each layer, and UEs, respectively.

The phase shift of the m -th scattering element on the ℓ -th metasurface layer is denoted as $\phi_m^{(\ell)} = \alpha_m^{(\ell)} e^{j\theta_m^{(\ell)}}$, where $\alpha_m^{(\ell)}$ and $\theta_m^{(\ell)}$ are the amplitude and phase shift, respectively, such that $\alpha_m^{(\ell)} = 1$ and $\theta_m^{(\ell)} \in [0, 2\pi)$, $\forall m \in \mathcal{M}, \forall \ell \in \mathcal{L}$. Moreover, we assume discrete phase shifts, where the interval $[0, 2\pi)$ is uniformly quantized into 2^b levels, with b denoting the number of quantization bits. The set of discrete phase shifts is defined as $\mathcal{B} = \{0, \Delta_\theta, 2\Delta_\theta, \dots, (2^b - 1)\Delta_\theta\}$, where $\Delta_\theta = 2\pi/2^b$. Thus, the phase-shift $\theta_m^{(\ell)}$ is quantized to the nearest values in \mathcal{B} as follows:

$$\begin{aligned} \theta_m^{(\ell)} &\leftarrow \arg \min_{\theta \in \mathcal{B}} |\theta - \theta_m^{(\ell)}|, \\ &= \Delta_\theta \left\lfloor \frac{\theta_m^{(\ell)}}{\Delta_\theta} + \frac{1}{2} \right\rfloor, \forall m \in \mathcal{M}, \forall \ell \in \mathcal{L}. \end{aligned} \quad (1)$$

Moreover, the phase shifts matrix of the ℓ -th metasurface layer is defined as

$$\Theta_\ell = \text{diag} \left(e^{j\theta_1^{(\ell)}}, e^{j\theta_2^{(\ell)}}, \dots, e^{j\theta_M^{(\ell)}} \right) \in \mathbb{C}^{M \times M}. \quad (2)$$

According to Rayleigh-Sommerfeld's diffraction theory [2], [37], we can obtain the propagation channel matrix between the $(\ell - 1)$ -th layer and ℓ -th layer which is denoted by $\mathbf{W}^{(\ell)} \in \mathbb{C}^{M \times M}$, $\ell = 2, \dots, L$. The (i, j) -th entry of $\mathbf{W}^{(\ell)}$ can be written as

$$w_{i,j}^{(\ell)} = \frac{d_x d_y d_{\text{Layer}}}{d_{i,j}^{(\ell)2}} \left(\frac{1}{2\pi d_{i,j}^{(\ell)}} - \frac{1}{\lambda} j \right) e^{j2\pi d_{i,j}^{(\ell)}/\lambda}, \quad (3)$$

where λ is the wavelength, d_x and d_y are the length and width of each RIS element, and $d_{i,j}^{(\ell)}$ is the transmission distance between j -th scattering element of $(\ell - 1)$ -th layer to the i -th scattering element of the ℓ -th layer. We assume the spacing between each layer is the same and it is denoted by d_{Layer} .

The propagation channel matrix from BS to the first metasurface layer is denoted by $\mathbf{W}^{(1)} = [\mathbf{w}_1, \dots, \mathbf{w}_N] \in \mathbb{C}^{M \times N}$ and can be obtained by replacing $d_{i,j}^{(\ell)}$ with $d_{i,n}^{(1)}$ and d_{Layer} with d_t , where d_t is the distance between the BS and the first

metasurface layer [2]. The wave-based beamforming matrix of the SIM-assisted system can be written as

$$\mathbf{G}_\vartheta = \left(\prod_{k=1}^{L-1} \Theta_{L+1-k} \mathbf{W}^{(L+1-k)} \right) \Theta_1 \in \mathbb{C}^{M \times M}. \quad (4)$$

The channel matrix from the last metasurface layer to the UEs is denoted by $\mathbf{H} = [\mathbf{h}_1, \dots, \mathbf{h}_K] \in \mathbb{C}^{M \times K}$, where $\mathbf{h}_K^H \in \mathbb{C}^{1 \times M}$, $\forall K$ is the SIM-UE channel vector which can be written as

$$\mathbf{h}_k = \sqrt{\beta_k} \mathbf{R}_{\text{RIS}}^{1/2} \mathbf{q}_{h_k}, \quad (5)$$

where $\mathbf{q}_{h_k} \sim \mathcal{CN}(0, \mathbf{1}_M)$ follows the Rayleigh fading distribution and $\sqrt{\beta_k}$ is the distance-dependent path loss corresponding to the SIM-UE channels. Furthermore, we assume far-field propagation in an isotropic scattering environment and $\mathbf{R}_{\text{RIS}} \in \mathbb{C}^{M \times M}$ denotes the deterministic Hermitian-symmetric positive semi-definite correlation matrix at the RIS in which the (i, j) -th term is given by

$$\mathbf{R}_{\text{RIS}, i, j} = \text{sinc} \left(\frac{2\sqrt{d_{i,j}^{(H)2} + d_{i,j}^{(V)2}}}{\lambda} \right), \quad (6)$$

where $d_{i,j}^{(H)}$ and $d_{i,j}^{(V)}$ represent the horizontal and vertical distances, respectively, between the m -th and j -th meta-atoms located on the same metasurface layer [1], [2].

In downlink transmission, we assume that each data stream related to each UE transmits from a corresponding BS antenna, which means the BS needs to select a suitable number of BS antennas in advance for the \mathcal{K} UE set. For simplicity, we assume $N = K$. Specifically, the k -th UE treats signals intended for the other UEs as interference. However, we use wave-based beamforming with the aid of SIM. Thus, we can adjust \mathbf{G} by optimizing phase shifts to mitigate interference. Let $s_k \in \mathbb{C}$ be the information symbol intended for the k -th UE with $\mathbb{E}\{|s_k|^2\} = 1$, i.e., unit-energy constellation, and $p_k > 0$ be the power allocation for the k -th UE. Therefore, total power constraint can be expressed as follows

$$\sum_{k=1}^K p_k \leq P_T, \quad (7)$$

where P_T is the power budget at the BS. The composite received signal at the k -th UE after superimposing all the signals through SIM assumes

$$r_k = \sqrt{p_k} \mathbf{h}_k^H \mathbf{G}_\vartheta \mathbf{w}_k s_k + \sum_{\substack{j=1 \\ j \neq k}}^K \sqrt{p_j} \mathbf{h}_k^H \mathbf{G}_\vartheta \mathbf{w}_j s_j + n_k, \forall k \in \mathcal{K}, \quad (8)$$

where $n_k \sim \mathcal{CN}(0, \sigma^2)$ denotes the complex white Gaussian noise.

III. JOINT POWER ALLOCATION AND WAVE-BASED BEAMFORMING WITH THE INSTANTANEOUS CSI

A. PROBLEM FORMULATION

In this section, our objective is to maximize the minimum per-UE achievable rate by jointly optimizing the transmit

power allocation and the wave-based beamforming at the SIM under instantaneous CSI. The SINR at k th UE can be expressed as

$$\gamma_k = \frac{|\mathbf{h}_k^H \mathbf{G}_\vartheta \mathbf{w}_k|^2 p_k}{\sum_{\substack{j=1 \\ j \neq k}}^K |\mathbf{h}_k^H \mathbf{G}_\vartheta \mathbf{w}_j|^2 p_j + \sigma^2}, \forall k \in \mathcal{K}. \quad (9)$$

Therefore, the achievable rate of the k -th UE is

$$R_k = \log_2(1 + \gamma_k), \forall k \in \mathcal{K}. \quad (10)$$

Since $\log_2(1 + \gamma_k)$ is a monotonically increasing function of $\gamma_k \geq 0$, the corresponding optimization problem can be formulated as

$$(P1) : \max_{\mathbf{p}, \vartheta} \min_{k \in \mathcal{K}} \frac{|\mathbf{h}_k^H \mathbf{G}_\vartheta \mathbf{w}_k|^2 p_k}{\sum_{\substack{j=1 \\ j \neq k}}^K |\mathbf{h}_k^H \mathbf{G}_\vartheta \mathbf{w}_j|^2 p_j + \sigma^2}, \quad (11a)$$

$$\text{subject to} \quad \sum_{k=1}^K p_k \leq P_T, \quad (11b)$$

$$p_k > 0, \forall k \in \mathcal{K}, \quad (11c)$$

$$\theta_m^{(\ell)} \in \mathcal{B}, \forall m \in \mathcal{M}, \forall \ell \in \mathcal{L}, \quad (11d)$$

where $\mathbf{p} = [p_1, p_2, \dots, p_K]^T \in \mathbb{R}^{K \times 1}$, $\boldsymbol{\theta}_\ell = [\theta_1^{(\ell)}, \theta_2^{(\ell)}, \dots, \theta_M^{(\ell)}]^T \in \mathbb{R}^{M \times 1}$ and $\boldsymbol{\vartheta} = [\boldsymbol{\theta}_1^T, \boldsymbol{\theta}_2^T, \dots, \boldsymbol{\theta}_L^T]^T \in \mathbb{R}^{ML \times 1}$.

The optimization problem (P1) is non-convex due to the coupling of \mathbf{p} and $\boldsymbol{\vartheta}$ in its objective function and restricted discrete values for $\theta_m^{(\ell)}$ in the constraint 13b. Thus, standard methods cannot be used to find a globally optimal solution. To address this, we propose an algorithm which decomposes the problem (P1) into two sub-problems. Additionally, we propose to solve the above-mentioned two sub-problems alternatively to obtain a sub-optimal solution described in the section III-B.

B. THE PROPOSED ALTERNATING OPTIMIZATION ALGORITHM

In this section, we describe the proposed alternating optimization algorithm for solving the max-min SINR optimization problem. Specifically, we solve the power allocation problem in the first sub-problem and the wave-based beamforming problem in the second sub-problem, as listed below.

- The power allocation optimization problem for fixed SIM phase shifts can be formulated as

$$(P2) : \max_{\mathbf{p}} \min_{k \in \mathcal{K}} \frac{|\mathbf{h}_k^H \mathbf{G}_\vartheta \mathbf{w}_k|^2 p_k}{\sum_{\substack{j=1 \\ j \neq k}}^K |\mathbf{h}_k^H \mathbf{G}_\vartheta \mathbf{w}_j|^2 p_j + \sigma^2}, \quad (12a)$$

$$\text{subject to} \quad \sum_{k=1}^K p_k \leq P_T, \quad (12b)$$

$$p_k > 0, \forall k \in \mathcal{K}. \quad (12c)$$

- The optimal wave-based beamforming problem for a given power allocation can be formulated as

$$(P3) : \max_{\boldsymbol{\vartheta}} \min_{k \in \mathcal{K}} \frac{|\mathbf{h}_k^H \mathbf{G}_\vartheta \mathbf{w}_k|^2 p_k}{\sum_{\substack{j=1 \\ j \neq k}}^K |\mathbf{h}_k^H \mathbf{G}_\vartheta \mathbf{w}_j|^2 p_j + \sigma^2}, \quad (13a)$$

$$\text{subject to} \quad \theta_m^{(\ell)} \in \mathcal{B}, \forall m \in \mathcal{M}, \forall \ell \in \mathcal{L}. \quad (13b)$$

Algorithm 1 Max-Min SINR Optimization.

- 1: **Initialization:** Set $i = 1$. Initialize the SIM phase shifts $\boldsymbol{\theta}_\ell = \mathbf{0}, \forall \ell \in \mathcal{L}$.
 - 2: Solve the optimization problem (P2) and find the optimal power allocation for the i -th iteration for the given $\boldsymbol{\theta}_\ell \forall \ell \in \mathcal{L}$.
 - 3: Solve the optimization problem (P3) and find the optimal SIM phase shifts for the i -th iteration for the given \mathbf{P} .
 - 4: Repeat steps 2 and 3 until convergence.
 - 5: $i = i + 1$.
-

Thus, we propose a two-stage algorithm to solve the optimization problem (P1) as presented in the algorithm 1.

1) *Optimal Power Allocation With Given $\boldsymbol{\vartheta}$* : Specifically, we can reformulate the optimization problem (P2) in epigraph form by introducing an auxiliary variable t as follows [38],

$$(P2.1): \max_{t \geq 0, \mathbf{p}} t \quad (14a)$$

$$\text{subject to } t \leq \frac{|\mathbf{h}_k^H \mathbf{G}_{\boldsymbol{\vartheta}} \mathbf{w}_k|^2 p_k}{\sum_{\substack{j=1 \\ j \neq k}}^K |\mathbf{h}_k^H \mathbf{G}_{\boldsymbol{\vartheta}} \mathbf{w}_j|^2 p_j + \sigma^2}, \forall k \in \mathcal{K}, \quad (14b)$$

$$\text{constraints (12b), (12c).} \quad (14c)$$

The problem (P2.1) can be rewritten as

$$(P2.2): \max_{t \geq 0, \mathbf{p}} t \quad (15a)$$

$$\text{subject to } \sum_{\substack{j=1 \\ j \neq k}}^K s_{k,j} p_j + \sigma_k^2 \leq \frac{s_{k,k}}{t}, \forall k \in \mathcal{K}, \quad (15b)$$

$$\text{constraints (12b), (12c).} \quad (15c)$$

where $s_{k,k} = |\mathbf{h}_k^H \mathbf{G}_{\boldsymbol{\vartheta}} \mathbf{w}_j|^2$. Thus, the objective function and the constraints are monomial and polynomial functions. Hence, the optimization problem (P2.2) follows the standard form of the GP problem [38], and it can be solved using standard optimization tools.

2) *Optimal Wave-Based Beamforming With Given \mathbf{p}* : We propose a GDA-based algorithm to solve the wave-based beamforming optimization problem described below. Here, we relaxed the discrete phase shifts into the continuous domain. Thereby, we transform the optimization problem (P3), by introducing an auxiliary vector variable $\boldsymbol{\lambda} = [\lambda_1, \dots, \lambda_K]^T \in \mathbb{R}^{K \times 1}$ and $\Lambda = \{\boldsymbol{\lambda} | \lambda_k \geq 0, \forall k, \mathbf{1}^T \boldsymbol{\lambda} = 1\}$ as follows:

$$(P3.1): \max_{\boldsymbol{\vartheta}} \min_{\boldsymbol{\lambda}} \sum_{k=1}^K \frac{\lambda_k |\mathbf{h}_k^H \mathbf{G}_{\boldsymbol{\vartheta}} \mathbf{w}_k|^2 p_k}{\sum_{\substack{j=1 \\ j \neq k}}^K |\mathbf{h}_k^H \mathbf{G}_{\boldsymbol{\vartheta}} \mathbf{w}_j|^2 p_j + \sigma^2}, \quad (16a)$$

$$\text{subject to } \boldsymbol{\lambda} \geq 0, \mathbf{1}^T \boldsymbol{\lambda} = 1, \quad (16b)$$

$$\text{constraints (13b).} \quad (16c)$$

The equivalence of Problem (P3) and Problem (P3.1) arises from the fact that, for a fixed $\boldsymbol{\vartheta}$, we assign $\lambda_k = 1$ for the minimum and $\lambda_i = 0, i \neq k$ for the rest [30].

$$\text{Let us define } f(\boldsymbol{\lambda}, \boldsymbol{\vartheta}) = \sum_{k=1}^K \frac{\lambda_k |\mathbf{h}_k^H \mathbf{G}_{\boldsymbol{\vartheta}} \mathbf{w}_k|^2 p_k}{\sum_{\substack{j=1 \\ j \neq k}}^K |\mathbf{h}_k^H \mathbf{G}_{\boldsymbol{\vartheta}} \mathbf{w}_j|^2 p_j + \sigma^2}.$$

Therefore, for fixed $\boldsymbol{\vartheta}$, the auxiliary variable $\boldsymbol{\lambda}$ can be updated by applying a projection gradient descent step as follows:

$$\bar{\boldsymbol{\lambda}}^{(i+1)} = \boldsymbol{\lambda}^{(i)} - \epsilon \cdot \nabla_{\boldsymbol{\lambda}} f(\boldsymbol{\lambda}^{(i)}, \boldsymbol{\vartheta}^{(i)}), \quad (17a)$$

$$\boldsymbol{\lambda}^{(i+1)} = \arg \min_{\mathbf{y} \in S_{\boldsymbol{\lambda}}} \|\mathbf{y} - \bar{\boldsymbol{\lambda}}^{(i+1)}\|_2^2, \quad (17b)$$

where ϵ is the step size and $S_{\boldsymbol{\lambda}} = \{\mathbf{y} | \mathbf{y} \in \mathbb{R}^{K \times 1}, \mathbf{y} \geq 0, \mathbf{1}_K^T \mathbf{y} = 1\}$. Moreover $\nabla_{\boldsymbol{\lambda}} f = \left[\frac{\partial f}{\partial \lambda_1}, \dots, \frac{\partial f}{\partial \lambda_K} \right]^T$ is the gradient of f with respect to $\boldsymbol{\lambda}$ where $\frac{\partial f}{\partial \lambda_k}$ can be obtained as follows:

$$\frac{\partial f}{\partial \lambda_k} = \sum_{k=1}^K \frac{\partial \lambda_k \gamma_k}{\partial \lambda_k} = \gamma_k. \quad (18)$$

The projection operation in (17b) can be effectively solved using the Karush-Kuhn-Tucker (KKT) conditions since the optimization problem (17b) exhibits convexity. Therefore, its Lagrangian function can be written as follows.

$$L(\mathbf{y}, \boldsymbol{\xi}, \eta) = \|\mathbf{y} - \bar{\boldsymbol{\lambda}}^{(i+1)}\|_2^2 + \boldsymbol{\xi}^T (-\mathbf{y}) + \eta (\mathbf{1}_K^T \mathbf{y} - 1), \quad (19)$$

where $\boldsymbol{\xi} \in \mathbb{R}^{K \times 1}$ and $\eta \in \mathbb{R}$ are the Lagrange multipliers. We can obtain the KKT conditions as listed below.

- $\nabla_{\mathbf{y}} (L(\mathbf{y}, \boldsymbol{\xi}^*, \eta^*))$ vanishes at \mathbf{y}^* :

$$\mathbf{y}^* = \bar{\boldsymbol{\lambda}}^{(i+1)} + \frac{1}{2} (\boldsymbol{\xi}^* - \eta^* \mathbf{1}_K). \quad (20)$$

- Prime feasibility:

$$\bar{\boldsymbol{\lambda}}^{(i+1)} \geq \frac{1}{2} (\eta^* \mathbf{1}_K - \boldsymbol{\xi}^*), \quad (21a)$$

$$K \eta^* = \mathbf{1}_K^T (\boldsymbol{\xi}^* + 2 \bar{\boldsymbol{\lambda}}^{(i+1)}) - 2. \quad (21b)$$

- Dual feasibility:

$$\boldsymbol{\xi}^* \geq 0. \quad (22)$$

- Complementary slackness: Using (21a) and (22),

$$\boldsymbol{\xi}^* = \max(\eta^* \mathbf{1}_K - 2 \bar{\boldsymbol{\lambda}}^{(i+1)}, \mathbf{0}). \quad (23)$$

Here, $\boldsymbol{\xi}^*, \eta^*$, and \mathbf{y}^* are the optimal solutions for the problem (19). With the help of (23), we can define $\boldsymbol{\xi}^* + 2 \bar{\boldsymbol{\lambda}}^{(i+1)} = \max(\eta^* \mathbf{1}_K, 2 \bar{\boldsymbol{\lambda}}^{(i+1)})$. According to (21b), we can further define

$$g(\eta) = \mathbf{1}_K^T \cdot \max(\eta^* \mathbf{1}_K, 2 \bar{\boldsymbol{\lambda}}^{(i+1)}) - 2. \quad (24)$$

$g(\eta)$ is monotonic in η and $\frac{2}{K} \mathbf{1}_K^T \bar{\boldsymbol{\lambda}}^{(i+1)} - \frac{2}{K} \leq \eta^* \leq 2 \max_k \bar{\lambda}_k^{(i+1)}$. Therefore, we can find a solution for η^* using bisection search until predefined accuracy ϵ is achieved. Thus, for a given η^* , we can find optimal $\boldsymbol{\xi}^*$ and \mathbf{y}^* and then we can update $\boldsymbol{\lambda}^{(i+1)}$.

Moreover, for fixed $\boldsymbol{\lambda}$, all the SIM phase shifts $\boldsymbol{\vartheta}$ can be updated using gradient ascent step as follows:

$$\bar{\boldsymbol{\vartheta}}^{(i+1)} = \boldsymbol{\vartheta}^{(i)} + \mu \cdot \nabla_{\boldsymbol{\vartheta}} f(\boldsymbol{\lambda}^{(i+1)}, \boldsymbol{\vartheta}^{(i)}), \quad (25a)$$

$$\boldsymbol{\vartheta}^{(i+1)} = \arg \min_{\mathbf{b} \in S_{\boldsymbol{\vartheta}}} \|\mathbf{x} - \bar{\boldsymbol{\vartheta}}^{(i+1)}\|_2^2, \quad (25b)$$

where $S_{\boldsymbol{\vartheta}} = \{\mathbf{x} | \mathbf{x} \in \mathbb{R}^{ML \times 1}, x_i \in [0, 2\pi)\}$. Here, μ is the step size which is updated using a backtracking line search [38]. Specifically, $\nabla_{\boldsymbol{\vartheta}} f =$

Algorithm 2 Gradient Descent-Ascent Algorithm.

Input: $\{\mathbf{W}^{(\ell)}\}_{\ell=1}^L$, $\{\mathbf{h}_k^H\}_{k=1}^K$, \mathbf{p} , κ_1 , τ , ε , ν_1 , and maximum number of iterations (I_{max}).

- 1: **Initialization:** Set $i = 1$, $\boldsymbol{\vartheta}^{(1)} = \mathbf{0}$, $\mu = 1$, $\epsilon = 1$, and $\boldsymbol{\lambda}^{(1)} = \frac{1}{K}\mathbf{1}$.
- 2: **for** $i = 1$ to I_{max} **do**
- 3: According to (17), Update $\boldsymbol{\lambda}^{(i+1)}$.
- 4: **while**
 $f(\boldsymbol{\lambda}^{(i+1)}, \boldsymbol{\vartheta}^{(i)} + \mu \cdot \nabla_{\boldsymbol{\vartheta}} f(\boldsymbol{\lambda}^{(i+1)}, \boldsymbol{\vartheta}^{(i)})) < f(\boldsymbol{\lambda}^{(i+1)}, \boldsymbol{\vartheta}^{(i)}) + \nu_1 \mu \nabla_{\boldsymbol{\vartheta}} f(\boldsymbol{\lambda}^{(i+1)}, \boldsymbol{\vartheta}^{(i)})^T \nabla_{\boldsymbol{\vartheta}} f(\boldsymbol{\lambda}^{(i+1)}, \boldsymbol{\vartheta}^{(i)})$
do
- 5: $\mu = \kappa_1 \mu$.
- 6: **end while**
- 7: According to (25), update $\boldsymbol{\vartheta}^{(i+1)}$.
- 8: Let $\epsilon \leftarrow \tau \mu$.
- 9: **Until** Convergence or $i \geq I_{max}$
- 10: **end for**

Output: Optimal $\boldsymbol{\vartheta}$.

$\left[\frac{\partial f}{\partial \theta_1^{(1)}}, \dots, \frac{\partial f}{\partial \theta_M^{(1)}}, \dots, \frac{\partial f}{\partial \theta_1^{(L)}}, \dots, \frac{\partial f}{\partial \theta_M^{(L)}} \right]^T$ is the gradient of f with respect to $\boldsymbol{\vartheta}$, where $\frac{\partial f}{\partial \theta_m^{(\ell)}}$ is obtained in the following lemma.

Lemma 1: The gradient of the objective function f with respect to the phase shift $\theta_m^{(\ell)}$ at the m -th element of the ℓ -th metasurface layer is given by:

$$\frac{\partial f}{\partial \theta_m^{(\ell)}} = \sum_{k=1}^K \lambda_k \omega_k \left(p_k \delta_{m,k,k}^{(\ell)} - \gamma_k \sum_{\substack{j=1 \\ j \neq k}}^K p_j \delta_{m,k,j}^{(\ell)} \right), \quad (26)$$

where $\delta_{m,k,j}^{(\ell)}$ and ω_k are defined as

$$\delta_{m,k,j}^{(\ell)} = 2\Im \left[e^{-j\theta_m^{(\ell)}} \mathbf{w}_j^H \mathbf{a}_m^{\ell} (\mathbf{b}_m^{\ell})^H \mathbf{h}_k \mathbf{h}_k^H \mathbf{G}_{\boldsymbol{\vartheta}} \mathbf{w}_j \right], \quad (27)$$

$$\omega_k = \frac{1}{\sum_{\substack{j=1 \\ j \neq k}}^K |\mathbf{h}_k^H \mathbf{G}_{\boldsymbol{\vartheta}} \mathbf{w}_j|^2 p_j + \sigma^2}, \quad (28)$$

with $(\mathbf{a}_m^{\ell})^H$ and \mathbf{b}_m^{ℓ} denoting the m -th row of $\mathbf{A}_{\ell} \in \mathbb{C}^{M \times M}$ and the m -th column of $\mathbf{B}_{\ell} \in \mathbb{C}^{M \times M}$, in which \mathbf{A}_{ℓ} and \mathbf{B}_{ℓ} are defined as

$$\mathbf{A}_{\ell} \triangleq \begin{cases} \mathbf{W}^{(\ell)} \boldsymbol{\Theta}_{\ell-1} \cdots \boldsymbol{\Theta}_2 \mathbf{W}^{(2)} \boldsymbol{\Theta}_1, & \text{if } \ell \neq 1, \\ \mathbf{I}_M & \text{if } \ell = 1, \end{cases} \quad (29)$$

and

$$\mathbf{B}_{\ell} \triangleq \begin{cases} \boldsymbol{\Theta}_L \mathbf{W}^{(L)} \boldsymbol{\Theta}_{L-1} \cdots \boldsymbol{\Theta}_{\ell+1} \mathbf{W}^{(\ell+1)}, & \text{if } \ell \neq L, \\ \mathbf{I}_M, & \text{if } \ell = L, \end{cases} \quad (30)$$

respectively.

Proof: Please, refer to Appendix A. \blacksquare

The GDA algorithm is summarized in Algorithm 2. Specifically, when selecting step sizes, we follow the two-time scale GDA method explained in [39]. Thus, we follow that $\epsilon > \mu$ since the minimization step should dominate the maximization step. Therefore, we update $\epsilon = \tau \mu$ where $\tau > 0$. After obtaining optimal values for $\boldsymbol{\vartheta}$, we finally quantize $\theta_m^{(\ell)}$ into values in \mathcal{B} according to the quantization operation mentioned in (1).

The computational complexity of GDA algorithm is $\mathcal{O}(I_{GDA} [LMK^2(4M+3) + K + \log(\varepsilon^{-1})])$. Also, the computational complexity of GP is $\mathcal{O}(K^{\frac{7}{2}})$ [31]. Thus, total computational complexity is $\mathcal{O}(I_{AO} (K^{\frac{7}{2}} + I_{GDA} [LMK^2(4M+3) + K + \log(\varepsilon^{-1})]))$, where I_{GDA} and I_{AO} are the iteration need to converge the GDA algorithm and alternating optimization algorithm, respectively. Moreover, the computational complexity of the exhaustive search algorithm is $\mathcal{O}(2^{bML})$, which is significantly higher than the complexity of the proposed algorithm.

IV. JOINT POWER ALLOCATION AND WAVE-BASED BEAMFORMING WITH THE STATISTICAL CSI

In this section, our main focus is on maximizing the average minimum achievable rate when statistical CSI is available at the SIM. The advantage of leveraging statistical CSI is the reduction of computational and signaling overhead compared to instantaneous CSI, making SIM optimization more practical for real-world applications. To be specific, the channel covariance matrix \mathbf{R}_{RIS} is assumed to be known to the SIM. Against this backdrop, let us denote the minimum SINR among the K users as

$$\gamma_{\min}(\boldsymbol{\vartheta}, \mathbf{p}) = \min(\gamma_1, \gamma_2, \dots, \gamma_K), \quad (31)$$

from which we obtain the average minimum achievable rate as

$$R(\boldsymbol{\vartheta}, \mathbf{p}) = \mathbb{E} \{ \log_2(1 + \gamma_{\min}(\boldsymbol{\vartheta}, \mathbf{p})) \}, \quad (32)$$

where the mathematical expectation is taken with respect to the distribution of γ_{\min} . Consequently, we may write the

corresponding stochastic optimization problem as

$$(P4) : \max_{\mathbf{p}, \boldsymbol{\vartheta}} \mathbb{E} \{ \log_2 (1 + \gamma_{\min}(\boldsymbol{\vartheta}, \mathbf{p})) \}, \quad (33a)$$

$$\text{subject to } \sum_{k=1}^K p_k \leq P_T, \quad (33b)$$

$$p_k > 0, \forall k \in \mathcal{K}, \quad (33c)$$

$$\theta_m^{(\ell)} \in \mathcal{B}, \forall m \in \mathcal{M}, \forall \ell \in \mathcal{L}. \quad (33d)$$

The above problem, in its current form, is intractable due to the expectation operator in the objective function. Therefore, to facilitate further analysis, we need to evaluate this quantity. To this end, noting that

$$\gamma_k = \frac{|\mathbf{h}_k^H \mathbf{G}_{\boldsymbol{\vartheta}} \mathbf{w}_k|^2 p_k}{\sum_{\substack{j=1 \\ j \neq k}}^K |\mathbf{h}_k^H \mathbf{G}_{\boldsymbol{\vartheta}} \mathbf{w}_j|^2 p_j + \sigma^2} \quad (34)$$

are independent random variables, for $k \in \mathcal{K}$, the cumulative distribution function (CDF) of γ_{\min} can be written as

$$\begin{aligned} F_{\gamma_{\min}}(z; \boldsymbol{\vartheta}, \mathbf{p}) &= 1 - \prod_{k=1}^K \Pr \{ \gamma_k > z \} \\ &= 1 - \prod_{k=1}^K (1 - F_{\gamma_k}(z; \boldsymbol{\vartheta}, \mathbf{p})), \end{aligned} \quad (35)$$

where $F_{\gamma_k}(z; \boldsymbol{\vartheta}, \mathbf{p})$ denotes the CDF of γ_k . Therefore, we may use the integration by parts technique to rewrite $\mathbb{E} \{ \log_2 (1 + \gamma_{\min}(\boldsymbol{\vartheta}, \mathbf{p})) \}$ as

$$\begin{aligned} \mathbb{E} \{ \log_2 (1 + \gamma_{\min}(\boldsymbol{\vartheta}, \mathbf{p})) \} \\ = \log_2 e \int_0^\infty \frac{\prod_{k=1}^K (1 - F_{\gamma_k}(z; \boldsymbol{\vartheta}, \mathbf{p}))}{1 + z} dz. \end{aligned} \quad (36)$$

Clearly, the main challenge here is to determine the CDF of γ_k . This stems from the fact that both the numerator and the denominator of γ_k depend on the random vector \mathbf{h}_k and thereby they are correlated. This is further exacerbated by the rank deficiency of the matrix $\sum_{\substack{j=1 \\ j \neq k}}^K \mathbf{w}_j \mathbf{w}_j^H p_j$, which in

turn makes the vector $\left(\sum_{\substack{j=1 \\ j \neq k}}^K \mathbf{w}_j \mathbf{w}_j^H p_j \right)^{1/2} \mathbf{G}_{\boldsymbol{\vartheta}}^H \mathbf{h}_k$ Gaussian distributed, however with a *singular* covariance matrix. Moreover, bounding techniques akin to what is given in [40] (i.e., use-and-then-forget bound) are not applicable, since we are not considering large antenna arrays. Therefore, for analytical tractability, we may upper bound γ_k as $\gamma_k < \tilde{\gamma}_k$, where

$$\tilde{\gamma}_k = |\mathbf{h}_k^H \mathbf{G}_{\boldsymbol{\vartheta}} \mathbf{w}_k|^2 \frac{p_k}{\sigma^2}. \quad (37)$$

It is also noteworthy that $\tilde{\gamma}_k$ can be interpreted as the SNR.

The stochastic inequality $\gamma_k < \tilde{\gamma}_k$ implies $F_{\gamma_k}(z; \boldsymbol{\vartheta}, \mathbf{p}) > F_{\tilde{\gamma}_k}(z; \boldsymbol{\vartheta}, \mathbf{p})$, $\forall \boldsymbol{\vartheta}, \mathbf{p}$. Therefore, following (36), we conveniently obtain an upper bound on the average minimum rate as

$$\begin{aligned} \mathbb{E} \{ \log_2 (1 + \gamma_{\min}(\boldsymbol{\vartheta}, \mathbf{p})) \} \\ = \log_2 e \int_0^\infty \frac{\prod_{k=1}^K (1 - F_{\gamma_k}(z; \boldsymbol{\vartheta}, \mathbf{p}))}{1 + z} dz \\ < \log_2 e \int_0^\infty \frac{\prod_{k=1}^K (1 - F_{\tilde{\gamma}_k}(z; \boldsymbol{\vartheta}, \mathbf{p}))}{1 + z} dz. \end{aligned} \quad (38)$$

Now noting that $\mathbf{h}_k^H \mathbf{G}_{\boldsymbol{\vartheta}} \mathbf{w}_k \sim \mathcal{CN}(0, \beta_k \mathbf{w}_k^H \mathbf{G}_{\boldsymbol{\vartheta}}^H \mathbf{R}_{\text{RIS}} \mathbf{G}_{\boldsymbol{\vartheta}} \mathbf{w}_k)$, we may write the CDF of $\tilde{\gamma}_k$ as

$$F_{\tilde{\gamma}_k}(z; \boldsymbol{\vartheta}, \mathbf{p}) = 1 - \exp \left(- \frac{\sigma^2 z}{\beta_k p_k \mathbf{w}_k^H \mathbf{G}_{\boldsymbol{\vartheta}}^H \mathbf{R}_{\text{RIS}} \mathbf{G}_{\boldsymbol{\vartheta}} \mathbf{w}_k} \right). \quad (39)$$

Consequently, we obtain from (38)

$$\begin{aligned} \mathbb{E} \{ \log_2 (1 + \gamma_{\min}(\boldsymbol{\vartheta}, \mathbf{p})) \} \\ < \log_2 e \int_0^\infty \frac{\exp(-\sigma^2 \zeta(\boldsymbol{\vartheta}, \mathbf{p}) z)}{1 + z} dz, \end{aligned} \quad (40)$$

where

$$\zeta(\boldsymbol{\vartheta}, \mathbf{p}) = \sum_{k=1}^K \frac{1}{\beta_k p_k \mathbf{w}_k^H \mathbf{G}_{\boldsymbol{\vartheta}}^H \mathbf{R}_{\text{RIS}} \mathbf{G}_{\boldsymbol{\vartheta}} \mathbf{w}_k}. \quad (41)$$

Alternatively, one can rewrite (40) as

$$\mathbb{E} \{ \log_2 (1 + \gamma_{\min}(\boldsymbol{\vartheta}, \mathbf{p})) \} < \log_2 e \mathbb{E} \left\{ \frac{1}{\zeta(\boldsymbol{\vartheta}, \mathbf{p}) \sigma^2 + z} \right\}, \quad (42)$$

where the expectation is taken with respect to an exponential random variable with the density function $\exp(-z)$, $z \geq 0$. Therefore, having motivated with the above bounding process, to facilitate further analysis, we may consider an alternative problem given by

$$(P5) : \max_{\mathbf{p}, \boldsymbol{\vartheta}} \mathbb{E} \left\{ \frac{1}{\zeta(\boldsymbol{\vartheta}, \mathbf{p}) \sigma^2 + z} \right\}, \quad (43a)$$

$$\text{subject to } \sum_{k=1}^K p_k \leq P_T, \quad (43b)$$

$$p_k > 0, \forall k \in \mathcal{K}, \quad (43c)$$

$$\theta_m^{(\ell)} \in \mathcal{B}, \forall m \in \mathcal{M}, \forall \ell \in \mathcal{L}. \quad (43d)$$

A careful inspection of the above problem reveals that it is an alternative formulation corresponding to the maximization of the average minimum achievable rate given by

$$\tilde{R}(\boldsymbol{\vartheta}, \mathbf{p}) = \mathbb{E} \{ \log_2 (1 + \tilde{\gamma}_{\min}(\boldsymbol{\vartheta}, \mathbf{p})) \}, \quad (44)$$

where $\tilde{\gamma}_{\min}(\boldsymbol{\vartheta}, \mathbf{p}) = \min(\tilde{\gamma}_1, \tilde{\gamma}_2, \dots, \tilde{\gamma}_K)$. Here, the notable difference is that we consider the SNR instead of the SINR. This approach, however with the instantaneous CSI, has been adopted in [30]. Therefore, we obtain an optimistic average minimum rate in comparison with the case corresponding to the SINR. Nevertheless, as our simulation results reveal, this bound serves as a good approximation for the true average rate in the low SNR regime. The utility of this approach should be viewed in conjunction with the extreme analytical complexity associated with the original problem involving the SINR. Furthermore, our proposed approach reduces the complexity of the original optimization since it does not require updating the policy in every coherence interval.

Now, keeping in mind that $\mathbb{E} \left\{ \frac{1}{\zeta(\boldsymbol{\vartheta}, \mathbf{p}) \sigma^2 + z} \right\}$ is convex and decreasing in $\zeta(\boldsymbol{\vartheta}, \mathbf{p})$ [38], the problem (P5) can equivalently be written as

$$(P6) : \min_{\mathbf{p}, \boldsymbol{\vartheta}} \sum_{k=1}^K \frac{1}{\beta_k p_k \mathbf{w}_k^H \mathbf{G}_{\boldsymbol{\vartheta}}^H \mathbf{R}_{\text{RIS}} \mathbf{G}_{\boldsymbol{\vartheta}} \mathbf{w}_k}, \quad (45a)$$

$$\text{subject to } \sum_{k=1}^K p_k \leq P_T, \quad (45b)$$

$$p_k > 0, \forall k \in \mathcal{K}, \quad (45c)$$

$$\theta_m^{(\ell)} \in \mathcal{B}, \forall m \in \mathcal{M}, \forall \ell \in \mathcal{L}. \quad (45d)$$

The optimal policies corresponding to the above problem (P6), given by $\mathbf{p} = \tilde{\mathbf{p}}^*$ and $\boldsymbol{\vartheta} = \tilde{\boldsymbol{\vartheta}}^*$, yield the maximum of the minimum achievable rate

$$\begin{aligned} \tilde{R}(\tilde{\boldsymbol{\vartheta}}^*, \tilde{\mathbf{p}}^*) &= \log_2 e \mathbb{E} \left\{ \frac{1}{\zeta(\tilde{\boldsymbol{\vartheta}}^*, \tilde{\mathbf{p}}^*) \sigma^2 + z} \right\} \\ &= \exp \left(\zeta(\tilde{\boldsymbol{\vartheta}}^*, \tilde{\mathbf{p}}^*) \sigma^2 \right) E_1 \left(\zeta(\tilde{\boldsymbol{\vartheta}}^*, \tilde{\mathbf{p}}^*) \sigma^2 \right), \end{aligned} \quad (46)$$

where $E_1(z) = \int_z^\infty \frac{\exp(-t)}{t} dt$, $z > 0$ is the exponential function. Consequently, we can relate the above rate to the desired optimal rate corresponding to the original stochastic optimization problem (P4) as

$$R(\boldsymbol{\vartheta}^*, \mathbf{p}^*) < \tilde{R}(\tilde{\boldsymbol{\vartheta}}^*, \tilde{\mathbf{p}}^*), \quad (47)$$

where $\mathbf{p} = \mathbf{p}^*$ and $\boldsymbol{\vartheta} = \boldsymbol{\vartheta}^*$ are the optimal policies for the original problem (P4).

Having been motivated by the above reasoning, we now focus on determining the optimal policies for the problems (P5) and (P6). We propose an alternating optimization algorithm to solve the problem (P6). Specifically, we solve the power allocation problem in the first sub-problem and the wave-based beamforming problem in the second sub-problem, as listed below. We solve these two sub-problems iteratively until convergence to find $\tilde{\mathbf{p}}^*$ and $\tilde{\boldsymbol{\vartheta}}^*$ similarly as the Algorithm 1.

- The power allocation optimization problem for fixed SIM phase shifts can be formulated as

$$(P6.1) : \min_{\mathbf{p}} \sum_{k=1}^K \frac{1}{\beta_k p_k \mathbf{w}_k^H \mathbf{G}_{\boldsymbol{\vartheta}}^H \mathbf{R}_{\text{RIS}} \mathbf{G}_{\boldsymbol{\vartheta}} \mathbf{w}_k}, \quad (48a)$$

$$\text{subject to constraints (45b), (45c).} \quad (48b)$$

Thus, the objective function and the constraints are monomial and polynomial functions. Hence, the optimization problem (P6.1) follows the standard form of the GP problem [38], and it can be solved using standard optimization tools.

- The optimal wave-based beamforming problem for a given power allocation can be formulated as

$$(P6.2) : \min_{\boldsymbol{\vartheta}} \sum_{k=1}^K \frac{1}{\beta_k p_k \mathbf{w}_k^H \mathbf{G}_{\boldsymbol{\vartheta}}^H \mathbf{R}_{\text{RIS}} \mathbf{G}_{\boldsymbol{\vartheta}} \mathbf{w}_k}, \quad (49a)$$

$$\text{subject to constraints (45d).} \quad (49b)$$

Algorithm 3 Gradient Descent Algorithm.

Input: $\{\mathbf{W}^{(\ell)}\}_{\ell=1}^L$, \mathbf{R}_{RIS} , \mathbf{p} , κ_2 , ν_2 , and I_{max} .

- 1: **Initialization:** Set $i = 1$, $\boldsymbol{\vartheta}^{(1)} = \mathbf{0}$, $\iota = 1$.
- 2: **for** $i = 1$ to I_{max} **do**
- 3: **while** $\zeta(\mathbf{P}, \boldsymbol{\vartheta}^{(i)} - \iota \cdot \nabla_{\boldsymbol{\vartheta}} \zeta(\mathbf{P}, \boldsymbol{\vartheta}^{(i)})) > \zeta(\mathbf{P}, \boldsymbol{\vartheta}^{(i)}) - \nu_2 \iota \nabla_{\boldsymbol{\vartheta}} \zeta(\mathbf{P}, \boldsymbol{\vartheta}^{(i)})^T \nabla_{\boldsymbol{\vartheta}} \zeta(\mathbf{P}, \boldsymbol{\vartheta}^{(i)})$ **do**
- 4: $\iota = \kappa_2 \iota$
- 5: **end while**
- 6: According to (50), update $\boldsymbol{\vartheta}^{(i+1)}$.
- 7: **Until** Convergence or $i \geq I_{max}$
- 8: **end for**

Output: Optimal $\boldsymbol{\vartheta}$.

We propose a gradient descent-based algorithm to solve the wave-based beamforming optimization problem. Thus, all the SIM phase shifts $\boldsymbol{\vartheta}$ can be updated using gradient descent step as follows:

$$\boldsymbol{\vartheta}^{(i+1)} = \boldsymbol{\vartheta}^{(i)} - \iota \cdot \nabla_{\boldsymbol{\vartheta}} \zeta(\mathbf{P}, \boldsymbol{\vartheta}^{(i)}). \quad (50)$$

Here, ι is the step size which is updated using a backtracking line search [38]. Specifically, $\nabla_{\boldsymbol{\vartheta}} \zeta = \left[\frac{\partial \zeta}{\partial \theta_1^{(1)}}, \dots, \frac{\partial \zeta}{\partial \theta_M^{(1)}}, \dots, \frac{\partial \zeta}{\partial \theta_1^{(L)}}, \dots, \frac{\partial \zeta}{\partial \theta_M^{(L)}} \right]^T$ is the gradient of ζ with respect to $\boldsymbol{\vartheta}$, where $\frac{\partial \zeta}{\partial \theta_m^{(\ell)}}$ is obtained as follows.

Lemma II: The gradient of the objective function ζ , defined in (41), with respect to the phase shift $\theta_m^{(\ell)}$ at the m -th element of the ℓ -th metasurface layer is given by:

$$\frac{\partial \zeta}{\partial \theta_m^{(\ell)}} = \sum_{k=1}^K \frac{1}{\beta_k p_k} \frac{-c_{m,k}^{(\ell)}}{\left(\sum_{i=1}^M \rho_i |\mathbf{v}_i^H \mathbf{G}_{\boldsymbol{\vartheta}} \mathbf{w}_k|^2 \right)^2}, \quad (51)$$

where

$$c_{m,k}^{(\ell)} = 2 \sum_{i=1}^M \rho_i \Im \left[e^{-j\theta_m^{(\ell)}} (\mathbf{w}_k)^H \mathbf{a}_m^\ell (\mathbf{b}_m^\ell)^H \mathbf{v}_i \mathbf{v}_i^H \mathbf{G}_{\boldsymbol{\vartheta}} \mathbf{w}_k \right], \quad (52)$$

with ρ_i and \mathbf{v}_i denoting, respectively, the eigenvalues and eigenvectors of \mathbf{R}_{RIS} .

Proof: Please refer to Appendix B. ■

The gradient descent algorithm to find optimal $\boldsymbol{\vartheta}$ is described in Algorithm 3. After obtaining optimal values for $\tilde{\boldsymbol{\vartheta}}^*$, we finally quantize $\theta_m^{(\ell)}$ into values in \mathcal{B} using the quantization operation in 1. The total computational complexity of the alternating algorithm is $\mathcal{O} \left(I_{AO} \left(K^{\frac{7}{2}} + I_{GD} [LMK(4M^2 + 2M + 1)] \right) \right)$, where I_{GD} and I_{AO} are the iterations need to converge the gradient descent algorithm and alternating optimization algorithm, respectively.

V. NUMERICAL RESULTS

In this section, we provide simulation results to evaluate the performance of the proposed max-min SINR algorithm. Here, we consider a downlink of a SIM-assisted multi-user MIMO system. Fig. 2 shows an illustration of the simulation setup.

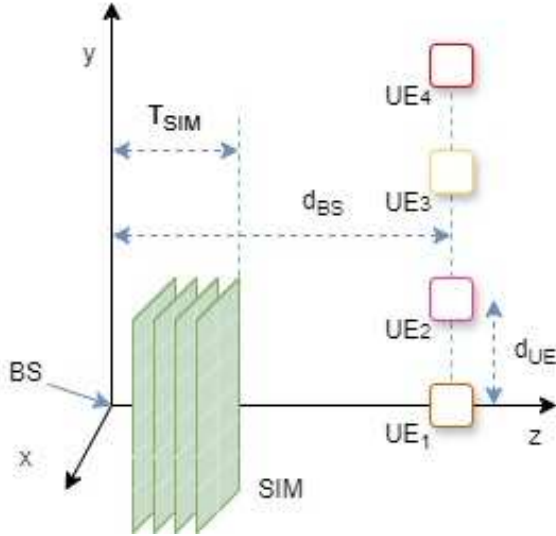


Fig. 2. Illustration of the simulation setup.

TABLE I
SIMULATION PARAMETERS

Carrier frequency, f_c	28 GHz
Length and width of each RIS element, d_x, d_y	$\lambda/2$
Thickness of SIM, T_{SIM}	5λ
The distance between UEs, d_{UE}	10 m
The perpendicular distance between BS and UE, d_{BS}	10 m
Free space path loss, C_0	-30 dB
The path loss exponent α	3.5
The reference distance, d_0	1 m
Noise variance for each UE, σ_k^2	-90 dBm

The BS has an M -antenna array along the x -axis, centred at $(0, 0, 0)$. Each SIM layer is positioned parallel to the x - y plane, and each layer's centre is aligned with the z -axis. The first SIM layer is spaced with T_{SIM}/L distance from the centre of the BS and the rest of the layers are spaced with T_{SIM}/L distance from each other, where T_{SIM} is the thickness of the SIM. UEs are located parallel to the y -axis, with perpendicular distance d_{BS} from the BS and d_{UE} distance between each UE. The distance-dependent path loss is modeled as

$$\beta_k = C_0(d_k/d_0)^{(-\alpha)}, d_k \geq d_0, \quad (53)$$

where $d_k = \sqrt{(d_{\text{BS}} - T_{\text{SIM}})^2 + (d_{\text{UE}}(k-1))^2}$ is the distance between SIM and k -th UE. Additionally, 5 dBi antenna gain is present at each antenna of the BS. Table I lists the rest of the simulation parameters.

A. JOINT POWER ALLOCATION AND WAVE-BASED BEAMFORMING WITH THE INSTANTANEOUS CSI

To the best of our knowledge, no other works have investigated a fairness-based resource allocation for a SIM-aided system. Thus, we compare the performance of the proposed max-min rate optimization algorithm based on instantaneous CSI with the standard approaches listed below.

- GP+GDA(Continuous phase shift): We solve the power allocation problem with GP and wave-based beamforming optimization algorithm for continuous phase shifts.

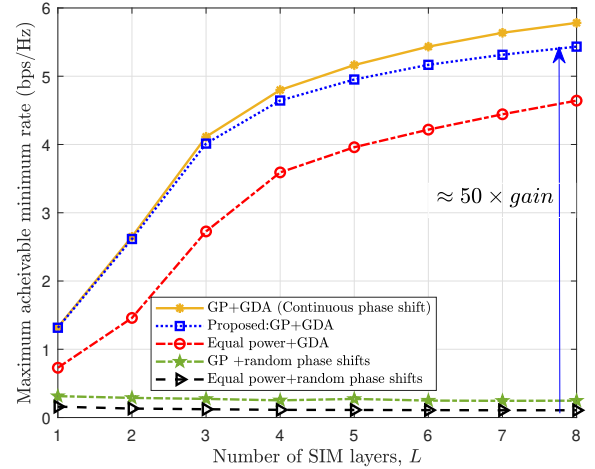


Fig. 3. The maximum achievable minimum data rate versus the number of SIM layers, L . The simulation is conducted with the parameters $N = K = 4$, $M = 36$, and $P_T = 10$ dBm.

- Proposed: (GP+GDA): The proposed max-min rate algorithm with instantaneous CSI using GP for power allocation and GDA algorithm with quantization for wave-based beamforming. Here, we use the parameters: $\kappa_1 = 0.8$, $\nu_1 = 0.3$, $\tau = 10$, $\varepsilon = 10^{-4}$, and $b = 8$.
- Equal power + GDA: We use equal power allocation between UEs by dividing the total power equally among UEs and the proposed GDA algorithm for wave-based beamforming optimization.
- GP + random phase shifts: We use optimal power allocation found using GP and randomly selected phase shift in \mathcal{B} .
- Equal power +random phase shift: We use equal power allocation between UEs and randomly selected phase shift in \mathcal{B} .

Fig. 3 shows the maximum achievable minimum rate variation with the number of SIM layers. It shows that the minimum rate increases with the number of SIM layers. Also, our proposed optimization scheme gives an approximate 50 times higher minimum rate than equal power allocation and random phase shift assignment. Further, our proposed algorithm can achieve an approximate 1.2 times higher minimum rate compared to equal power allocation with optimal phase shift assignment and an approximate 20 times higher minimum rate compared to optimal power allocation and random phase shift assignment when $L = 8$. Moreover, the minimum rate increases fourfold when compared to using one SIM layer with eight SIM layers, which proves the performance improvement capability of using SIM with multiple RIS layers. Additionally, the gap between our proposed optimization algorithm with quantization and continuous phase shift increases with the increase of SIM layers since the effect of quantization error increases with the increase in the number of phases that need to be optimized. However, the highest rate loss we observed due to the quantization is approximately 0.35 bps when $L = 8$.

The maximum achievable minimum rate variation with the number of RIS elements in each layer is shown in Fig. 4. It

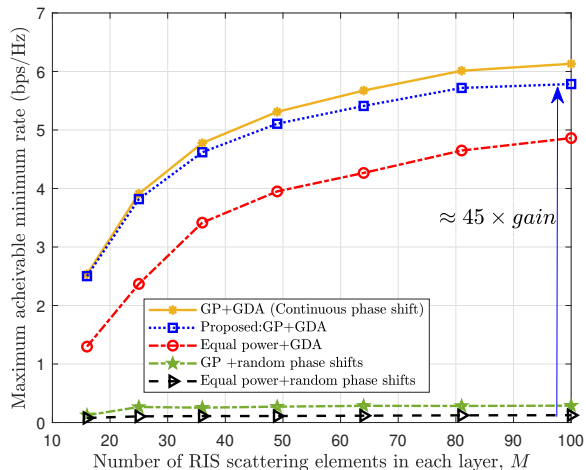


Fig. 4. The maximum achievable minimum data rate versus the number of scattering elements in each layer, M . The simulation is conducted with the parameters $N = K = 4$, $L = 4$, and $P_T = 10$ dBm.

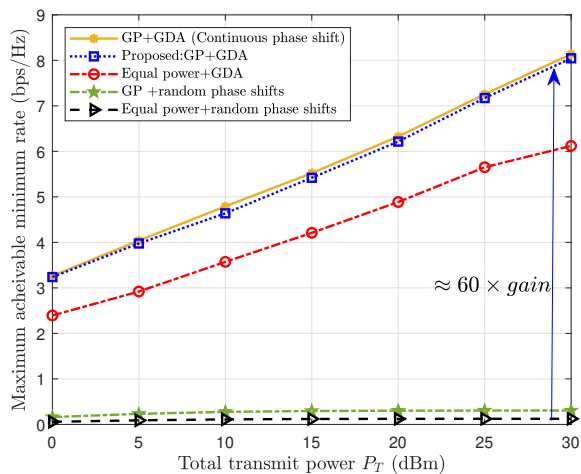


Fig. 5. The maximum achievable minimum data rate versus the total transmit power, P_T . The simulation is conducted with the parameters $N = K = 4$, $M = 36$, $L = 4$.

shows that the minimum rate increases with the number of RIS elements. Also, our proposed optimization scheme gives an approximate 45 times higher minimum rate than equal power allocation and random phase shift assignment. Further, our proposed algorithm can achieve an approximate 1.2 times higher minimum rate compared to equal power allocation with optimal phase shift assignment and an approximate 20 times higher minimum rate compared to optimal power allocation and random phase shift assignment when $M = 100$. Moreover, the gap between our proposed optimization algorithm with quantization and continuous phase shift increases with the increase of RIS elements since the effect of quantization error increases with the increase in the number of phases that need to be optimized. However, the highest rate loss we observed due to the quantization is approximately 0.35 bps when $M = 100$.

Fig. 5 shows the maximum achievable minimum rate variation with different total transmit power values for $L = 4$. They show that increased transmit power at the BS increases the minimum rate. Also, our proposed optimization scheme

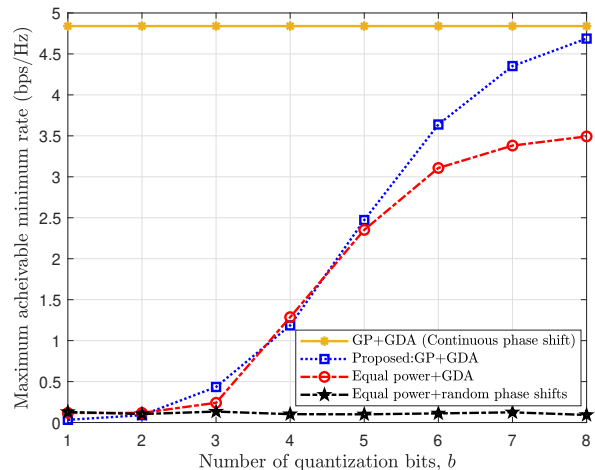


Fig. 6. The maximum achievable minimum data rate versus the number of quantization bits, b . The simulation is conducted with the parameters $N = K = 4$, $M = 36$, $L = 4$, and $P_T = 10$ dBm.

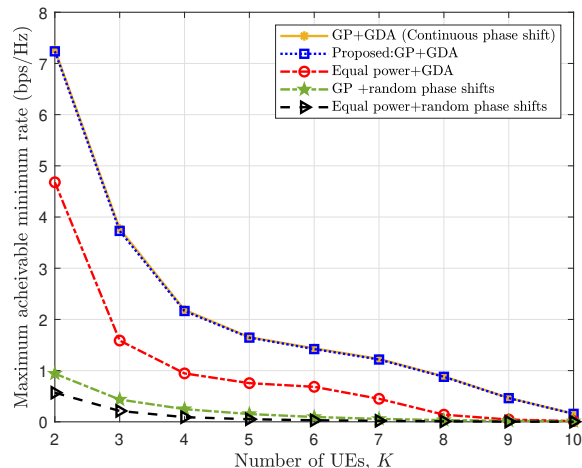


Fig. 7. The maximum achievable minimum data rate versus the number of UEs, K . The simulation is conducted with the parameters $N = 10$, $M = 36$, $L = 4$, and $P_T = 10$ dBm.

gives an approximate 60 times higher minimum rate than equal power allocation and random phase shift assignment. Further, our proposed algorithm can achieve an approximate 1.3 times higher minimum rate compared to equal power allocation with optimal phase shift assignment and an approximate 25 times higher minimum rate compared to optimal power allocation and random phase shift assignment when the total power at BS is 30 dBm and $M = 36$, $L = 4$. Moreover, the highest rate loss we observed due to the quantization is 0.1 bps.

Fig. 6 shows the performance variation of the algorithm for different numbers of bits used to quantize the phase shift. In Fig. 6, it is visible that when $b = 8$, our proposed algorithm achieved the performance of the GDA algorithm when we assume continuous phase shifts. Only a 0.1 bps rate loss occurs due to the quantization using 8 bits. However, due to the quantization error, the rate loss is high if b is 1 to 5.

The maximum achievable minimum rate variation with the

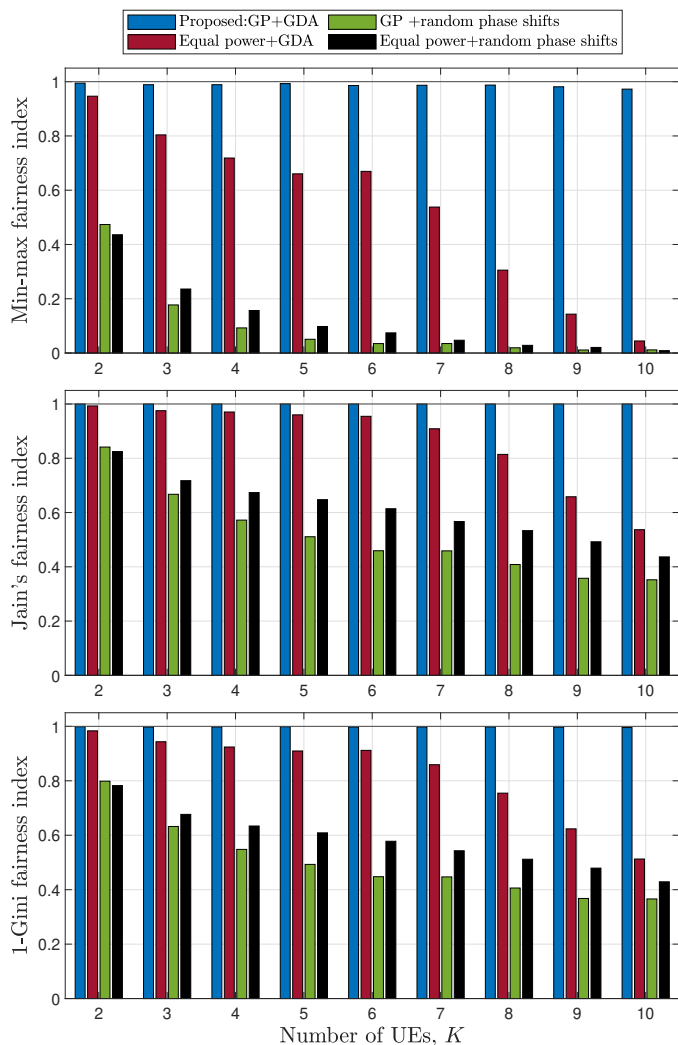


Fig. 8. The fairness index versus the number of UEs, K . The simulation is conducted with the parameters $N = 10$, $M = 36$, $L = 4$, and $P_T = 10$ dBm.

number of UEs is shown in Fig. 7. According to Fig. 7, the minimum rate decreases as the number of UEs grows since the limitation in power at the BS. Moreover, when the system has a very high number of UEs, i.e., $K > 5$, the system gives a very low minimum rate for the weaker UE. However, our proposed optimization scheme gives an approximate 15 times higher minimum rate than equal power allocation and random phase shift assignment, even for 10 UEs.

All the simulations in Section V-V-A are carried out for 1000 channel realizations. In summary, the proposed alternating optimization algorithm performs better with benchmark schemes: equal power allocation with GDA, GP power allocation with random phase shifts, equal power allocation with random phase shifts, and GP power allocation with exhaustive search. In addition, the proposed algorithm performs almost similarly to the GDA with continuous phase shift values when we quantize using 8 bits. Moreover, it is visible that finding optimal SIM phase shifts contributes more to improving performance than optimal power allocation.

To further investigate our proposed algorithm's performance,

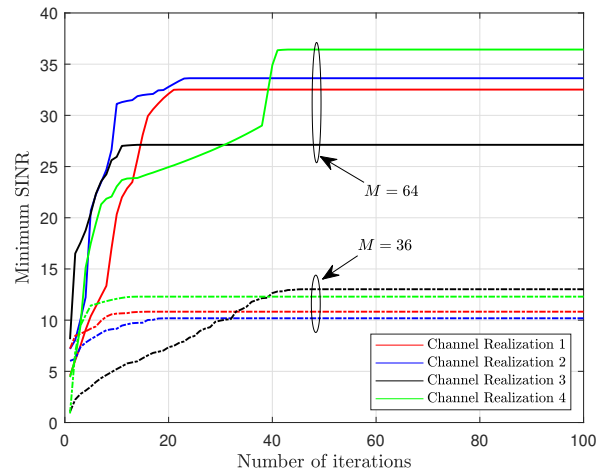


Fig. 9. Convergence behavior of max-min fairness alternating optimization algorithm with instantaneous CSI.

we analyze its resource allocation's fairness. Specifically, we utilize the following three fairness indices, which are frequently used in wireless communication systems [41]–[44] to analyze the fairness of our proposed methods as well as the used benchmark schemes.

$$\begin{aligned} \text{Min-max fairness index} \quad I_{\min-\max} &= \frac{\min(R_k)}{\max(R_k)}, \\ \text{Jain's fairness index} \quad I_{\text{Jain}} &= \frac{|\sum_{k=1}^K R_k|^2}{K \sum_{k=1}^K R_k^2}, \\ \text{Gini fairness index} \quad I_{\text{Gini}} &= \frac{1}{2K^2 \bar{R}} \sum_{i=1}^K \sum_{j=1}^K |R_i - R_j|, \end{aligned}$$

where $\bar{R} = (1/K) \sum_{j=1}^K R_j$ is the average rate. All three fairness indexes vary from 1 to 0. Both the min-max fairness and Jain's fairness indices result in a value of 1, indicating a high degree of fairness, whereas a value of 0 indicates complete unfairness. In contrast, the Gini fairness index results in a value of 0, indicating a high degree of fairness, whereas a value of 1 indicates complete unfairness. Therefore, here we consider $1 - I_{\text{Gini}}$ for ease of comparison. Fig. 8 shows the variation of the above-mentioned three fairness indices with the number of UEs for our proposed 'GP+GDA' max-min fairness algorithm and the benchmark schemes. According to Fig. 8, the proposed max-min fairness algorithm exhibits that the fairness indices are approximately equal to 1 even when the system has 10 UEs. This demonstrates that our proposed algorithm exhibits high fairness irrespective of the number of users. In contrast, the benchmark schemes show a reduction in fairness when the number of UEs grow. Thus, this proves that our proposed algorithm can allocate resources such that the system is highly fair for every UE.

Fig. 9 shows the convergence behavior of max-min fairness optimization algorithm with instantaneous CSI for the alternating optimization algorithm. It shows that the proposed algorithm converges in a reasonable number of iterations.

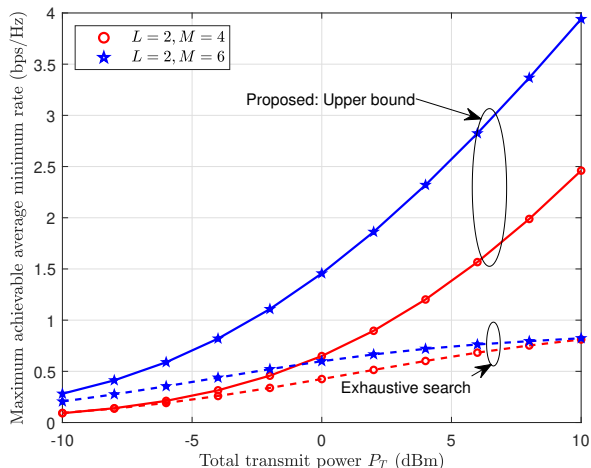


Fig. 10. The maximum achievable average minimum rate versus the total transmit power, P_T . The simulation is conducted with the parameters $N = K = 2$.

B. JOINT POWER ALLOCATION AND WAVE-BASED BEAMFORMING WITH THE STATISTICAL CSI

To the best of our knowledge, no other works have investigated a fairness-based resource allocation for a SIM-aided system. Thus, we compare the performance of the proposed max-min rate optimization algorithm based on statistical CSI with the standard approaches listed below.

- Proposed: Upper bound: The proposed algorithm to maximize the average minimum achievable rate with statistical CSI using GP programming for optimal power allocation and gradient descent algorithm with quantization for wave-based beamforming. Here, we use the parameters: $\kappa_2 = 0.8$, $\nu_2 = 0.3$, and $b = 3$.
- Exhaustive search: We solve the optimization problem (P4) with an exhaustive search algorithm when $b = 1$. Here, we assume total transmit power, P_T is a discrete variable with 0.01 resolution.

Fig. 10 compares our proposed upper bound and the results obtained exhaustively for the maximum achievable average minimum rate. Further, it shows the variation of the maximum achievable average minimum rate with transmit power. According to Fig. 10, it exhibits a tight upper bound for low transmit power at BS, in other words, during the low SNR regime. (Since we assume noise power is constant throughout this simulation). Thus, it proves the applicability of the proposed upper bound even if it is overly optimized in the high SNR regime. Therefore, we are able to reduce the frequency of finding optimal power allocation and wave-based beamforming using the proposed upper bound for statistical CSI. We have done this simulation for low L and M values due to the high complexity of the exhaustive algorithm.

The variation of the upper bound for the maximum achievable average minimum rate with transmit power and number of RIS elements at each SIM layer and number of SIM layers is shown in Fig. 11. According to Fig. 11, it exhibits an increase in the upper bound with the increase of P_T , L and M .

Fig. 12 shows the convergence behavior of max-min fairness

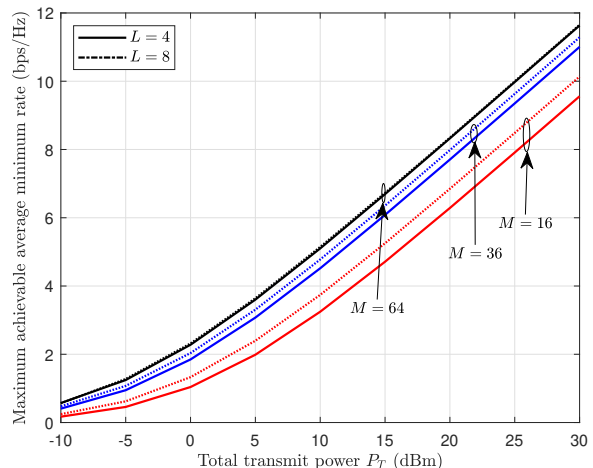


Fig. 11. The proposed upper bound for the maximum achievable average minimum rate versus the total transmit power at BS, P_T . The simulation is conducted with the parameters $N = K = 4$.

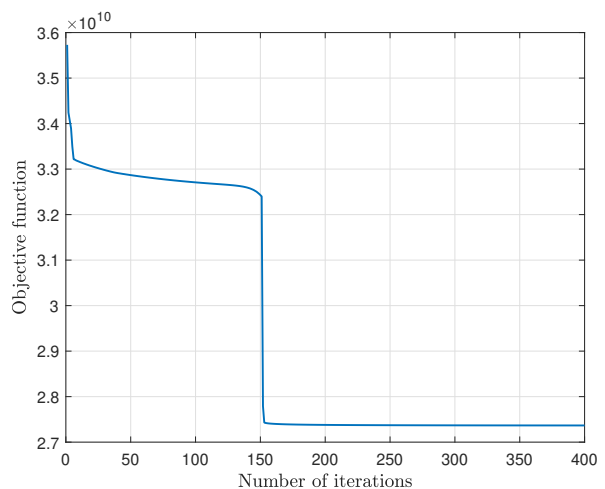


Fig. 12. Convergence behavior of max-min fairness alternating optimization algorithm with statistical CSI.

optimization algorithm with statistical CSI for the alternating optimization algorithm. It shows that the algorithm converges in a reasonable number of iterations.

VI. CONCLUSION

Max-min fairness optimization is crucial to guaranteeing fair performance for all users in a SIM-assisted multi-user system. In this paper, we proposed two novel max-min fairness algorithms based on instantaneous CSI and statistical CSI for SIM-assisted multi-user MISO systems. First, we propose a novel max-min fairness algorithm using alternating optimization technique to jointly optimize the power allocation and the wave-based beamforming based on instantaneous CSI. To this end, we utilize GP and gradient descent-ascent algorithms. Next, we proposed a novel algorithm to maximize the average minimum achievable rate based on statistical CSI, focusing on a bound on the average achievable rate, since an exact average rate is analytically intractable. Subsequent simulation

results demonstrate significant performance improvement due to the proposed optimization algorithms. These results further exhibit higher minimum rate than equal power allocation and random phase shift assignments for instantaneous CSI. Additionally, our simulations show that the proposed upper bound for the maximum achievable average minimum rate is tight for low SNR regime for statistical CSI. Thus, it is plausible to reduce computational overhead utilizing max-min fairness optimization in conjunction with the statistical CSI, since it eliminates the need to optimize during every coherence interval. Notwithstanding the above observation, though computationally not efficient, per coherent frame max-min optimization with instantaneous CSI gives better results.

APPENDIX A PROOF OF LEMMA I

The gradient of γ_k with respect to $\theta_m^{(\ell)}$ can be expressed as

$$\frac{\partial f}{\partial \theta_m^{(\ell)}} = \sum_{k=1}^K \lambda_k \frac{\partial \gamma_k}{\partial \theta_m^{(\ell)}}, \quad (\text{A-1})$$

Subsequently, using the derivative of the ratio of two differentiable functions, i.e., the quotient rule, we can obtain $\frac{\partial \gamma_k}{\partial \theta_m^{(\ell)}}$ as

$$\begin{aligned} \frac{\partial \gamma_k}{\partial \theta_m^{(\ell)}} &= \frac{p_k}{\sum_{j=1}^K |\mathbf{h}_k^H \mathbf{G}_\vartheta \mathbf{w}_j|^2 p_j + \sigma_k^2} \frac{\partial |\mathbf{h}_k^H \mathbf{G}_\vartheta \mathbf{w}_k|^2}{\partial \theta_m^{(\ell)}} \\ &\quad - \frac{|\mathbf{h}_k^H \mathbf{G}_\vartheta \mathbf{w}_k|^2 p_k}{(\sum_{j=1}^K |\mathbf{h}_k^H \mathbf{G}_\vartheta \mathbf{w}_j|^2 p_j + \sigma_k^2)^2} \sum_{j=1, j \neq k}^K p_j \frac{\partial |\mathbf{h}_k^H \mathbf{G}_\vartheta \mathbf{w}_j|^2}{\partial \theta_m^{(\ell)}}, \end{aligned} \quad (\text{A-2})$$

where $\frac{\partial |\mathbf{h}_k^H \mathbf{G}_\vartheta \mathbf{w}_j|^2}{\partial \theta_m^{(\ell)}}$ can be expressed as

$$\begin{aligned} \frac{\partial |\mathbf{h}_k^H \mathbf{G}_\vartheta \mathbf{w}_j|^2}{\partial \theta_m^{(\ell)}} &= \frac{\partial |\sum_{m=1}^M e^{j\theta_m^{(\ell)}} \mathbf{h}_k^H \mathbf{b}_m^{(\ell)} (\mathbf{a}_m^\ell)^H \mathbf{w}_j|^2}{\partial \theta_m^{(\ell)}}, \\ &= \frac{\partial \sum_{m=1}^M e^{j\theta_m^{(\ell)}} \mathbf{z}_{m,l,k,j} \sum_{m=1}^M e^{-j\theta_m^{(\ell)}} \mathbf{z}_{m,l,k,j}^*}{\partial \theta_m^{(\ell)}}, \\ &= j e^{j\theta_m^{(\ell)}} \mathbf{z}_{m,l,k,j} \sum_{m=1}^M e^{-j\theta_m^{(\ell)}} \mathbf{z}_{m,l,k,j}^* \\ &\quad + (-j) e^{-j\theta_m^{(\ell)}} \mathbf{z}_{m,l,k,j}^* \sum_{m=1}^M e^{j\theta_m^{(\ell)}} \mathbf{z}_{m,l,k,j}, \\ &\stackrel{\text{a}}{=} 2\Re \left[(-j) e^{-j\theta_m^{(\ell)}} \mathbf{z}_{m,l,k,j}^* \sum_{m=1}^M e^{j\theta_m^{(\ell)}} \mathbf{z}_{m,l,k,j} \right], \\ &= 2\Im \left[\left(e^{j\theta_m^{(\ell)}} \mathbf{h}_k^H \mathbf{b}_m^{(\ell)} (\mathbf{a}_m^\ell)^H \mathbf{w}_j \right)^H (\mathbf{h}_k^H \mathbf{G}_\vartheta \mathbf{w}_j) \right], \\ &= \delta_{m,k,j}^{(\ell)}, \end{aligned} \quad (\text{A-3})$$

where $\mathbf{z}_{m,l,k,j} = \mathbf{h}_k^H \mathbf{b}_m^{(\ell)} (\mathbf{a}_m^\ell)^H \mathbf{w}_j$. The step $\stackrel{\text{a}}{=}$ results from the fact that the gradient is real-valued. Substituting $\delta_{m,k,j}^{(\ell)}$ into the gradient expression and factoring out ω_k yields the final result, which completes the proof. \blacksquare

APPENDIX B PROOF OF LEMMA II

It seems intractable to obtain gradient of $\frac{1}{\beta_k p_k \mathbf{w}_k^H \mathbf{G}_\vartheta^H \mathbf{R}_{\text{RIS}} \mathbf{G}_\vartheta \mathbf{w}_k}$. Hence, we eigen decompose the \mathbf{R}_{RIS} as $\mathbf{R}_{\text{RIS}} = \sum_{i=1}^M \rho_i \mathbf{v}_i \mathbf{v}_i^H$ where ρ_i and \mathbf{v}_i are eigenvalues and eigenvectors of \mathbf{R}_{RIS} , respectively. Thus, it can be written that

$$\mathbf{w}_k^H \mathbf{G}_\vartheta^H \mathbf{R}_{\text{RIS}} \mathbf{G}_\vartheta \mathbf{w}_k = \sum_{i=1}^M \rho_i |\mathbf{v}_i^H \mathbf{G}_\vartheta \mathbf{w}_k|^2. \quad (\text{B-1})$$

Subsequently, using the derivative of the reciprocal of a function, i.e, reciprocal rule, we can express $\frac{\partial \zeta}{\partial \theta_m^{(\ell)}}$ as

$$\begin{aligned} \frac{\partial \zeta}{\partial \theta_m^{(\ell)}} &= \sum_{k=1}^K \frac{\partial}{\partial \theta_m^{(\ell)}} \left(\frac{1}{\beta_k p_k \mathbf{w}_k^H \mathbf{G}_\vartheta^H \mathbf{R}_{\text{RIS}} \mathbf{G}_\vartheta \mathbf{w}_k} \right), \\ &= \sum_{k=1}^K \frac{\partial}{\partial \theta_m^{(\ell)}} \left(\frac{1}{\beta_k p_k \sum_{i=1}^M \rho_i |\mathbf{v}_i^H \mathbf{G}_\vartheta \mathbf{w}_k|^2} \right), \\ &= \sum_{k=1}^K \frac{1}{\beta_k p_k} \frac{-\frac{\partial}{\partial \theta_m^{(\ell)}} \left(\sum_{i=1}^M \rho_i |\mathbf{v}_i^H \mathbf{G}_\vartheta \mathbf{w}_k|^2 \right)}{\left(\sum_{i=1}^M \rho_i |\mathbf{v}_i^H \mathbf{G}_\vartheta \mathbf{w}_k|^2 \right)^2}. \end{aligned} \quad (\text{B-2})$$

Next, by recalling Appendix A, we can express $\frac{\partial}{\partial \theta_m^{(\ell)}} \left(\sum_{i=1}^M \rho_i |\mathbf{v}_i^H \mathbf{G}_\vartheta \mathbf{w}_k|^2 \right)$ as

$$\begin{aligned} \frac{\partial}{\partial \theta_m^{(\ell)}} \left(\sum_{i=1}^M \rho_i |\mathbf{v}_i^H \mathbf{G}_\vartheta \mathbf{w}_k|^2 \right) &= \sum_{i=1}^M \rho_i \frac{\partial}{\partial \theta_m^{(\ell)}} (|\mathbf{v}_i^H \mathbf{G}_\vartheta \mathbf{w}_k|^2), \\ &= 2 \sum_{i=1}^M \rho_i \Im \left[e^{-j\theta_m^{(\ell)}} \mathbf{w}_k^H \mathbf{a}_m^\ell (\mathbf{b}_m^\ell)^H \mathbf{v}_i \mathbf{v}_i^H \mathbf{G}_\vartheta \mathbf{w}_k \right], \\ &= c_{m,k}^{(\ell)}. \end{aligned} \quad (\text{B-3})$$

Summing over all eigenmodes $i = 1, \dots, M$ and users $k = 1, \dots, K$, weighted by ρ_i and $\frac{1}{\beta_k p_k}$, yields the final expression for $\frac{\partial \zeta}{\partial \theta_m^{(\ell)}}$. This completes the proof. \blacksquare

REFERENCES

- [1] J. An, M. Di Renzo, M. Debbah, and C. Yuen, "Stacked intelligent metasurfaces for multiuser beamforming in the wave domain," in *2023 IEEE Int. Conf. Commun. (ICC)*, 2023, pp. 2834–2839.
- [2] J. An *et al.*, "Stacked intelligent metasurfaces for efficient holographic MIMO communications in 6G," *IEEE J. Sel. Areas Commun.*, vol. 41, no. 8, pp. 2380–2396, 2023.
- [3] M. Nerini and B. Clerckx, "Physically consistent modeling of stacked intelligent metasurfaces implemented with beyond diagonal RIS," *IEEE Commun. Lett.*, vol. 28, no. 7, pp. 1693–1697, 2024.
- [4] J. An *et al.*, "Stacked intelligent metasurface-aided MIMO transceiver design," *IEEE Wireless Commun.*, vol. 31, no. 4, pp. 123–131, 2024.
- [5] M. D. Renzo, "State-of-the-art on stacked intelligent metasurfaces: Communication, sensing and computing in the wave domain," 2024. [Online]. Available: <https://arxiv.org/abs/2411.19687>
- [6] Y.-F. Liu *et al.*, "A survey of recent advances in optimization methods for wireless communications," *IEEE J. Sel. Areas Commun.*, vol. 42, no. 11, pp. 2992–3031, 2024.
- [7] X. Lin, N. Shroff, and R. Srikant, "A tutorial on cross-layer optimization in wireless networks," *IEEE J. Sel. Areas Commun.*, vol. 24, no. 8, pp. 1452–1463, 2006.
- [8] C. W. Tan, "Wireless network optimization by perron-frobenius theory," in *2014 48th Annual Conference on Information Sciences and Systems (CISS)*, 2014, pp. 1–6.

- [9] M. Chiang, C. W. Tan, D. P. Palomar, D. O'Neill, and D. Julian, "Power control by geometric programming," *IEEE Trans. Wireless Commun.*, vol. 6, no. 7, pp. 2640–2651, 2007.
- [10] A. Sousa de Sena, M. Rasti, N. Huda Mahmood, and M. Latva-aho, "Beyond diagonal RIS for multi-band multi-cell MIMO networks: A practical frequency-dependent model and performance analysis," *IEEE Trans. Wireless Commun.*, vol. 24, no. 1, pp. 749–766, 2025.
- [11] B. Radunovic and J.-Y. Le Boudec, "A unified framework for max-min and min-max fairness with applications," *IEEE/ACM Trans. Netw.*, vol. 15, no. 5, pp. 1073–1083, 2007.
- [12] D. W. H. Cai, T. Q. S. Quek, and C. W. Tan, "A unified analysis of max-min weighted SINR for MIMO downlink system," *IEEE Trans. Signal Process.*, vol. 59, no. 8, pp. 3850–3862, 2011.
- [13] S. He, Y. Huang, L. Yang, A. Nallanathan, and P. Liu, "A multi-cell beamforming design by uplink-downlink max-min SINR duality," *IEEE Trans. Wireless Commun.*, vol. 11, no. 8, pp. 2858–2867, 2012.
- [14] A. Papazafeiropoulos, P. Kourtessis, S. Chatzinotas, D. I. Kaklamani, and I. S. Venieris, "Achievable rate optimization for large stacked intelligent metasurfaces based on statistical CSI," *IEEE Wireless Commun. Lett.*, vol. 13, no. 9, pp. 2337–2341, 2024.
- [15] J. An, M. D. Renzo, M. Debbah, H. V. Poor, and C. Yuen, "Stacked intelligent metasurfaces for multiuser downlink beamforming in the wave domain," 2023. [Online]. Available: <https://arxiv.org/abs/2309.02687>
- [16] A. Papazafeiropoulos, J. An, P. Kourtessis, T. Ratnarajah, and S. Chatzinotas, "Achievable rate optimization for stacked intelligent metasurface-assisted holographic MIMO communications," *IEEE Trans. Wireless Commun.*, vol. 23, no. 10, pp. 13 173–13 186, 2024.
- [17] Z. Li, J. An, and C. Yuen, "Stacked intelligent metasurfaces for fully-analog wideband beamforming design," in *2024 IEEE VTS Asia Pacific Wireless Communications Symposium (APWCS)*, 2024, pp. 1–5.
- [18] H. Liu, J. An, G. C. Alexandropoulos, D. W. K. Ng, C. Yuen, and L. Gan, "Multi-user MISO with stacked intelligent metasurfaces: a DRL-based sum-rate optimization approach," 2024. [Online]. Available: <https://arxiv.org/abs/2408.04837>
- [19] H. Liu, J. An, D. W. K. Ng, G. C. Alexandropoulos, and L. Gan, "DRL-based orchestration of multi-user MISO systems with stacked intelligent metasurfaces," in *ICC 2024 - IEEE International Conference on Communications*, 2024, pp. 4991–4996.
- [20] D. Darsena, F. Verde, I. Iudice, and V. Galdi, "Design of stacked intelligent metasurfaces with reconfigurable amplitude and phase for multiuser downlink beamforming," *IEEE Open Journal of the Communications Society*, vol. 6, pp. 531–550, 2025.
- [21] E. Shi, J. Zhang, Y. Zhu, J. An, C. Yuen, and B. Ai, "Harnessing stacked intelligent metasurface for enhanced cell-free massive MIMO systems: A low-power and cost approach," *arXiv preprint arXiv:2409.12851*, 2024.
- [22] S. Li, F. Zhang, T. Mao, R. Na, Z. Wang, and G. K. Karagiannidis, "Transmit beamforming design for ISAC with stacked intelligent metasurfaces," *IEEE Trans. Veh. Technol.*, pp. 1–6, 2024.
- [23] H. Cheng, J. Huang, G. Li, F. Wang, W. Hao, and S. Yang, "Max - min rate optimization for group- transmissive RIS- based transmitter architectures," in *2024 IEEE 99th Vehicular Technology Conference (VTC2024-Spring)*, 2024, pp. 1–5.
- [24] H. Xie, J. Xu, and Y.-F. Liu, "Max-min fairness in IRS-aided multi-cell MISO systems with joint transmit and reflective beamforming," *IEEE Trans. Wireless Commun.*, vol. 20, no. 2, pp. 1379–1393, 2021.
- [25] Q.-U.-A. Nadeem, A. Kammoun, A. Chaaban, M. Debbah, and M.-S. Alouini, "Asymptotic max-min SINR analysis of reconfigurable intelligent surface assisted MISO systems," *IEEE Trans. Wireless Commun.*, vol. 19, no. 12, pp. 7748–7764, 2020.
- [26] L. Cantos, M. Awais, and Y. H. Kim, "Max-min rate optimization for uplink IRS-NOMA with receive beamforming," *IEEE Wireless Commun. Lett.*, vol. 11, no. 12, pp. 2512–2516, 2022.
- [27] M. Bashar, K. Cumanan, A. G. Burr, P. Xiao, and M. Di Renzo, "On the performance of reconfigurable intelligent surface-aided cell-free massive MIMO uplink," in *GLOBECOM 2020 - 2020 IEEE Global Communications Conference*, 2020, pp. 1–6.
- [28] A. Subhash, A. Kammoun, A. Elzanaty, S. Kalyani, Y. H. Al-Badarneh, and M.-S. Alouini, "Max-min SINR optimization for RIS-aided uplink communications with green constraints," *IEEE Wireless Commun. Lett.*, vol. 12, no. 6, pp. 942–946, 2023.
- [29] W. Lai, Z. Wu, Y. Feng, K. Shen, and Y.-F. Liu, "An efficient convex-hull relaxation based algorithm for multi-user discrete passive beamforming," *IEEE Signal Process. Lett.*, vol. 31, pp. 2275–2279, 2024.
- [30] G. Yan, L. Zhu, and R. Zhang, "Passive reflector optimization for IRS-aided multicast beamforming with discrete phase shifts," *IEEE Wireless Commun. Lett.*, vol. 12, no. 8, pp. 1424–1428, 2023.
- [31] Q.-U.-A. Nadeem, A. Zappone, and A. Chaaban, "Achievable rate analysis and max-min SINR optimization in intelligent reflecting surface assisted cell-free MIMO uplink," *IEEE Open J. Commun. Soc.*, vol. 3, pp. 1295–1322, 2022.
- [32] A. Papazafeiropoulos, P. Kourtessis, and S. Chatzinotas, "Max-min SINR analysis of STAR-RIS assisted massive MIMO systems with hardware impairments," *IEEE Trans. Wireless Commun.*, vol. 23, no. 5, pp. 4255–4268, 2024.
- [33] D. Gunasinghe and G. Amarasinghe, "Statistical CSI based phase-shift and transmit power optimization for RIS-aided massive MIMO," in *GLOBECOM 2022 - 2022 IEEE Global Communications Conference*, 2022, pp. 4007–4012.
- [34] Z. Yu, Y. Han, M. Matthaiou, X. Li, and S. Jin, "Statistical CSI-based design for RIS-assisted communication systems," *IEEE Wireless Commun. Lett.*, vol. 11, no. 10, pp. 2115–2119, 2022.
- [35] K. Zhi, C. Pan, H. Ren, and K. Wang, "Statistical CSI-based design for reconfigurable intelligent surface-aided massive MIMO systems with direct links," *IEEE Wireless Commun. Lett.*, vol. 10, no. 5, pp. 1128–1132, 2021.
- [36] M. Eskandari, H. Zhu, A. Shojafard, and J. Wang, "Statistical CSI-based beamforming for RIS-aided multiuser MISO systems via deep reinforcement learning," *IEEE Wireless Commun. Lett.*, vol. 13, no. 2, pp. 570–574, 2024.
- [37] X. Lin *et al.*, "All-optical machine learning using diffractive deep neural networks," *Science*, vol. 361, no. 6406, pp. 1004–1008, 2018. [Online]. Available: <https://www.science.org/doi/abs/10.1126/science.aat8084>
- [38] S. Boyd and L. Vandenberghe, *Convex Optimization*. Cambridge, UK: Cambridge University Press, 2004.
- [39] T. Lin, C. Jin, and M. I. Jordan, "Two-timescale gradient descent ascent algorithms for nonconvex minimax optimization," *Journal of Machine Learning Research*, vol. 26, no. 11, pp. 1–45, 2025.
- [40] L. Sanguinetti, E. Björnson, and J. Hoydis, "Toward massive MIMO 2.0: Understanding spatial correlation, interference suppression, and pilot contamination," *IEEE Trans. Commun.*, vol. 68, no. 1, pp. 232–257, 2020.
- [41] M. Dianati, X. Shen, and S. Naik, "A new fairness index for radio resource allocation in wireless networks," in *IEEE Wireless Communications and Networking Conference, 2005*, vol. 2, 2005, pp. 712–717 Vol. 2.
- [42] R. K. Jain, D.-M. W. Chiu, W. R. Hawe *et al.*, "A quantitative measure of fairness and discrimination," *Eastern Research Laboratory, Digital Equipment Corporation, Hudson, MA*, vol. 21, no. 1, 1984.
- [43] U. U. Khan, N. Dilshad, M. H. Rehmani, and T. Umer, "Fairness in cognitive radio networks: Models, measurement methods, applications, and future research directions," *Journal of Network and Computer Applications*, vol. 73, pp. 12–26, 2016. [Online]. Available: <https://www.sciencedirect.com/science/article/pii/S1084804516301527>
- [44] Y. Cui, P. Liu, Y. Zhou, and W. Duan, "Energy-efficient resource allocation for downlink non-orthogonal multiple access systems," *Applied Sciences*, vol. 12, no. 19, 2022. [Online]. Available: <https://www.mdpi.com/2076-3417/12/19/9740>